UNIVERSITY OF CALIFORNIA

Los Angeles

Circular Secondary Clarifier Investigations Using a Numerical Model

A thesis submitted in partial satisfaction of the

Requirements for the degree Master of Science

in Civil Engineering

by

Andre Gharagozian

1998

The thesis of Andre Gharagozian is approved.

Thomas Harmon

Keith Stolzenbach

Russel Mau

Michael Stenstrom, Committee Chair

University of California, Los Angeles

~~1995~~ 1998

TABLE OF CONTENTS

LIST OF TABLES

LIST OF FIGURES

ACKNOWLEDGEMENTS

The author expresses his appreciation for the support, patience, and insightful review comments from his advisor, Michael K. Stenstrom, Chair of the Civil and Environmental Engineering Department at UCLA, California. The review comments from his thesis committee are also greatly appreciated. Special gratitude goes to Zdenko Cello Vitasovic of Reid Crowther Consulting Inc. in Seattle, Washington. Without the use of their model for research, the author would not have been able to perform this work. Eric J. Wahlberg from Brown and Caldwell in Pleasant Hill, California helped in identifying a specific topic to research. His input has been very helpful.

ABSTRACT OF THE THESIS

Circular Secondary Clarifier Investigations Using A Numerical Model

by

Andre Gharagozian

Master of Science in Civil Engineering

University of California, Los Angeles, 1998

Professor Michael K. Stenstrom, Chair

A two-dimensional finite-difference numerical model is used to simulate the hydraulic flow regime and to predict the effluent suspended solids (ESS) concentration in a circular secondary clarifier. One hundred and thirteen simulations are performed to evaluate the predicted ESS concentration as a function of the surface overflow rate (SOR) and the solids loading rate (SLR) for four different clarifier geometries. The four geometries are a shallow clarifier with a deep feed well skirt, a deep clarifier with a deep feed well skirt, a deep clarifier with a shallow feed well skirt, and a deep clarifier with no feed well skirt. For the shallow and deep clarifier with the deep feed well skirt, the model predicts that the ESS concentration is not sensitive to the SOR for overflow rates below 1 meter/hour (m/hr) to 1.5 m/hr (600 gal/ft^2/d-925 gal/ft^2/d). The ESS concentration is strongly dependent on the SLR within this SOR range. For the deep clarifiers with no feed well

skirt or a shallow skirt, the model predicts that the ESS concentration is highly sensitive to the SOR, and modestly sensitive to the SLR. The model also predicts that the ESS concentration is highly sensitive to the recirculation ratio (Influent Flow Rate/Return Activated Sludge Flow Rate). When the recirculation ratio is below 0.5, most of the simulations predicted clarifier failure with a rising sludge blanket. Conversely, with a recirculation ratio of above 0.5, the simulation reaches equilibrium quickly and predicts a high quality effluent (low suspended solids). The model agrees with field data presented by other authors. This model does not include interactions with the preceding aeration basin and may over predict process failure when compared to real situations.

INTRODUCTION

Secondary Clarifiers are extremely important to the activated sludge process, which is the most commonly used wastewater treatment system in the United States. Clarifiers are designed to remove the suspended solids in the effluent from activated sludge and other secondary treatment processes. When a clarifier does not perform well, an excessive amount of suspended solids escapes in the clarifier effluent. Besides being aesthetically unpleasant, the presence of solids can reduce the effectiveness of some disinfection processes. Also, effluent with high solids concentration can also have adverse impacts on receiving waters. A secondary function of clarifiers is to thicken the solids and return them back to the aeration process. When this does not happen, the biological mass in the aeration basin ultimately decreases along with the activated sludge process efficiency.

Current design criteria for secondary clarifiers only address the surface overflow rate (SOR) and the solids loading rate (SLR). Usually, specific geometrical criteria are not applied to designs. An exception to this are the "rule-of-thumb" approaches used to specify a clarifier's depth and baffle configurations.

Recent work Zhou *et al.* (1992b; 1992d), Vitasovic *et al.* (1997), and Wahlberg *et al.* (1997) address some of the geometry issues with circular secondary clarifiers along with the traditional design parameters of SOR and SLR criteria. Zhou *et al.* and Vitasovic *et*

al. perform their investigations with the aid of a numerical model that simulates the velocity and suspended solids concentration distributions for circular secondary clarifiers.

Using the same simulation model developed by Zhou *et al.* (1992b), the primary objectives of this thesis are to examine the effects the following parameters have on the effluent suspended solids (ESS) concentration of circular secondary clarifiers:

- SOR;
- SLR;
- clarifier depth; and
- feed well skirt depth.

The results of the simulations predict that the ESS concentration is sensitive to each of these parameters under different loading conditions and clarifier geometries. It is not sufficient to assert that as the SOR increases for a clarifier, so will its ESS concentration. The model predicts that for specific SOR ranges and clarifier geometries, the ESS is only weakly dependent on the SOR, and instead strongly dependent on the SLR. Conversely, there are clarifier geometries where the ESS is strongly dependent on the SOR, and only weakly dependent on the SLR. The work presented here attempts to identify some of these relationships.

BACKGROUND

Description

In the aeration basin of an activated sludge treatment process, microorganisms consume organic matter for energy and reproduction. As the organic matter is metabolized, the microorganisms grow and form biological flocs, or suspended solids.

Secondary clarifiers are circular or rectangular tanks designed to remove these biological flocs through gravity settling. Because secondary clarifiers are the primary removal mechanism for biological flocs, it is imperative that they be designed and operated properly so there is not an excess of suspended solids in the wastewater effluent.

The process flow arriving from an activated sludge process usually has a mixed liquor suspended solids (MLSS) concentration from 500 to 4,000 mg/L. As the influent flow enters the clarifier, the fluid velocity slows down and allows the solids (which are slightly more dense than water) to settle to the bottom. The solids, or sludge collected on the bottom are removed with a scraper or pipe withdrawal mechanism and has a solids concentration from 5,000 mg/L to 15,000 mg/L. Most of the solids are returned to the activated sludge aeration basin; a small fraction are disposed. The process flow leaving the clarifier or effluent passes over weirs near the top of the tank and has a suspended solids concentration of 5-30 mg/L if it is operating well to hundreds of mg/L if it is not.

In a center-feed circular clarifier, the influent flow enters through a vertical pipe in the center, and the effluent flows over weirs located near the clarifier perimeter. In a peripheral feed circular clarifier, the influent flow enters from the sides, and the effluent is withdrawn from the center.

Variables Affecting Clarifier Performance

The performance of a clarifier is typically defined in terms of the effluent suspended solids (ESS) concentration or by the degree of sludge thickening achieved. This paper discusses the efficiency in terms of the ESS concentration achieved. The performance efficiency of suspended solids removal is calculated using the expression below.

$$Efficiency = \frac{C_{influent} - C_{effluent}}{C_{influent}} \times 100\% \qquad (1)$$

Most clarifiers that operate properly should have an efficiency of at least 99%. There are several variables that affect a clarifier's suspended solids removal efficiency. The main variables are the following:

- solids settling characteristics;
- surface overflow rate (SOR);
- solids loading rate (SLR);
- hydrodynamic flow pattern;
- return activated sludge flow rate (RAS); and
- clarifier geometry.

The surface overflow rate is defined as the volumetric flow over the effluent weirs per unit clarifier surface area. This has been and still is the most widely used design parameter for determining the required area of a clarifier for a given influent flow (Metcalf and Eddy, 1991). Conceptually, the SOR is best described as the average upward flow velocity in the clarifier. For 50% of the solids particles to reach the bottom of a clarifier, its average particle settling velocity needs to be at least equal to the SOR. Typical SOR design criteria for secondary clarifiers are 0.6-1.3 m/hr (400 gal/ft^2/d-800 gal/ft^2/d) for average flow conditions, and no more than 2.0 m/hr (1,200 gal/ft^2/d) for peak hour flow conditions (Metcalf and Eddy 1991). The SOR is defined in equation two.

$$SOR = \frac{Q_{influent}}{A_{clarifier}} \qquad (2)$$

The influent flow is defined the actual flow into the clarifiers minus the recycle or return activated sludge (RAS) flow. This can also be conceptualized as the flow rate leaving the clarifier over the effluent weirs.

The solids loading rate is defined as the total solids mass entering the clarifier per unit time per unit clarifier surface area. The SLR is the second most widely used design parameter for determining the area of a clarifier. The maximum SLR that can be applied to a clarifier depends mostly on the solids settling characteristics. The higher the settling velocity is, the greater the maximum SLR. The SLR is defined in equation three.

$$SLR = \frac{\left(Q_{influent} + Q_{ras}\right) \times C_{influent}}{A_{clarifier}} \quad (3)$$

The solids settling characteristics strongly affects the solids distribution in the clarifier and the effluent suspended solids concentration. The settling characteristics depend mostly on the operating conditions of the activated sludge process preceding the clarifier (Wahlberg *et al.* 1994). Clearly, the denser the solids particles are, the faster they will settle. When solids concentrations are low, they will settle as discrete particles, independent of each other. As the concentration increases, the individual particle settling velocities decrease due to inter-particle forces. This is known as hindered settling. Also, there will always be a small, non-settling solids component in any flow coming from an activated sludge process. The magnitude of this non-settling component also depends primarily on the operating conditions in the preceding aeration basin.

The hydrodynamic flow pattern that develops inside a clarifier is often quite complicated and significantly affects the suspended solids distribution in the clarifier and the suspended solids concentration in the effluent. There is debate about whether a quiescent, non-turbulent flow or a slightly mixed clarifier is desired for optimum settling. A quiescent flow pattern will allow discrete particles to settle relatively undisturbed. A clarifier with some mixing will enhance flocculation (the growth of many smaller particles into fewer but larger particles), which can enhance settling if the fluid mixing is not too violent. Regardless of which type of flow pattern a clarifier has, three undesirable flow characteristics that undoubtedly increase the ESS concentration are dead zones,

short-circuiting, and excessive fluid velocity. Dead or stagnant zones are areas in a clarifier where the fluid does not exchange with the rest of the clarifier. This effectively reduces the residence time of the flow in the clarifier and reduces the settling efficiency. Short-circuiting occurs when a portion or all of the influent takes a shortened path to the effluent. This also reduces the residence time and the effective surface area. Excessive velocities can create a scouring effect on the sludge blanket in the bottom of the clarifier. The scouring of the sludge blanket resuspends the solids, which then may flow over the effluent weirs.

The hydraulic flow pattern in a clarifier is strongly dependent on the hydraulic load (HL). For this thesis, the hydraulic load will be defined as in equation four.

$$HL = \frac{Q_{inluent} + Q_{ras}}{A_{clarifier}} \tag{4}$$

The influent flow refers to the total flow entering the clarifier minus the return activated sludge flow. The hydraulic load refers to the flow rate entering the clarifier per unit area.

The volume of return activated sludge (RAS) withdrawn or the type of RAS withdrawal geometry used in a clarifier will affect the ESS concentration, the sludge blanket level in the clarifier, and the MLSS concentration in the preceding aeration basin. As the RAS flow rate increases, more solids are removed from the clarifier and returned to the aeration basin. This has the effect of lowering the sludge blanket level, which facilitates the clarification of the effluent. Increasing the RAS flow rate also has a negative effect

on sludge thickening. Because a greater volume of flow will be withdrawn from the clarifier bottom, the RAS concentration will not be as high. Another RAS process control variable is the location of the sludge withdrawal. Removing sludge near the effluent weirs may create a downward flux of solids in the effluent zone, which, may help clarify the liquid before it flows over the weirs. Samstag *et al.* (1992) investigated this phenomenon using field-testing and a numerical model, yet the results were inconclusive.

The appropriate clarifier geometry that will give the optimum solids removal efficiency is still debated. Some feel that a deep tank offers no advantages, and others feel that it is advantageous when sludge storage capacity is needed. Another parameter is the slope of the tank bottom. The slope can affect the density current that flows along the bottom of the clarifier. An optimal baffle and weir configuration effectively minimizes recirculation and short-circuiting. The influent feedwell baffle also helps to dissipate the influent flow energy and velocity to minimize scouring of the sludge blanket.

Clarifier Modeling Overview And Literature Review

Engineers and designers have attempted to predict or model a clarifier's suspended solids removal performance ever since their introduction as a wastewater treatment process in the late 1800's. The first accepted design criteria for predicting clarifier efficiency was the hydraulic residence or detention time. The clarifier volume divided by the effluent flow rate determines the hydraulic residence time. It was assumed that clarifiers would

perform adequately as long as the suspended solids were given enough time to settle. As early as 1904, Hazen (1904) provided evidence that removal of suspended solids depends on the surface area and not on the tank volume or the hydraulic residence time. In the last 50 years, the SOR has been the most useful design parameter for sizing a clarifier. However, analyzing or sizing a clarifier based only on its SOR value is a great simplification of what actually occurs in a clarifier. Most real clarifiers have complex mechanisms that affect suspended solids removal that are not addressed in a simple SOR analysis. Some of the mechanisms include:

- hydraulic recirculation;
- hydraulic short-circuiting;
- density waterfall in the inlet zone; and
- sludge blanket scouring due to high fluid velocities near the clarifier bottom.

The early pioneers of clarifier research understood this, but did not have the tools to analyze the complicated flow patterns that occur in clarifiers. In the last 10 years, there has been great progress in computational fluid dynamics, which has allowed researchers to analyze and predict the hydraulic and solids flow patterns in a clarifier with high accuracy. Some of these models are so accurate, that the hydraulic flow velocities and solids distributions consistently agree with field data after little calibration (Vitasovic *et al.* 1997). With such powerful tools, researchers can easily investigate the effect of varying one parameter while keeping all others constant. This is extremely difficult to do

when field testing clarifiers. Field testers do not have as much control over the input parameters as one has when using computational models. A good example of this is illustrated by the solids settling characteristics of the influent flow. It is rare for the settling characteristics to remain constant in an activated sludge process. So when data is collected over time, the researchers must be very careful to determine whether the observed trends are due to a change in the solids settling characteristics, or another process variable.

Dobbins (1943) describes the effect turbulence has on the suspended solids settling mechanisms for both discrete and flocculated particles. The discussion is limited to steady uniform flows in tanks or channels. Dobbins provides a detailed analytical analysis of one-dimensional sedimentation under turbulent conditions. He provides experimental results, which suggest that the sediment distribution follows a logarithmic distribution in the vertical axis. Dobbins' scope is not limited to sedimentation in clarifiers, but he makes a few observations that are important in understanding the settling mechanisms in clarifiers. The key points to his paper are listed below.

- The removal of discrete particles in a quiescent basin is independent of the depth of the settling basin.
- Solids resuspension due to scouring of the sludge blanket is dependent only on the hydraulic characteristics at the bottom.

Camp (1945) provides a collection of discussions on ten different aspects of sedimentation tank design. The author had created a thorough and current (in 1945)

account of settling tank theories and design criteria. Some of the important points he made are described below.

- The suspended solids removal rate is a function of the overflow rate and is independent of the tank depth and detention time.
- For discrete and flocculent particles, clarifier depths should be made as small as is consistent with no scouring of the sludge blanket.
- The density waterfall phenomenon is identified and a solution is recommended: Sludge withdrawn from the outlet end should alleviate the problem of the density current traveling up toward the effluent overflow weirs.
- Short-circuiting, dead zones, and other non-ideal hydraulic flow patterns are identified and described using tracer dye analysis techniques.

By 1945, Camp had already identified and addressed some very important issues in clarifier modeling. Many of these issues, particularly density-driven flows and hydraulic inefficiencies have been understood better in recent years with the help of computational fluid dynamics modeling.

TeKippe and Cleasby (1967) give an account of experiments which investigate the instabilities in peripheral feed model settling tanks. Large variations in the results of identical experiments were observed, especially at lower flow rates. The experimenters feel this can be explained by the difference in room temperature and the influent water temperature. Results were more reproducible when the room temperature and influent water temperature were of the same value, which suggests a strong correlation between clarifier stability and temperature gradients in the tank.

Schamber and Larock (1981) is an early attempt to model a clarifier. The authors developed a numerical model, which predicts the two-dimensional velocity field in primary sedimentation basins. The velocity field is determined from the Galerkin finite element solution of five coupled non-linear partial differential equations, which are the hydraulic mass and momentum transport equations. The two-equation kappa-epsilon model is used to determine the kinematic viscosity throughout the clarifier. The kinematic viscosity depends on the velocity field, and vice versa. The solids distribution is then determined once the velocity field is known. As one of the early efforts in clarifier modeling, this is an impressive accomplishment. However, because the authors were only concerned with primary sedimentation tanks with low suspended solids concentrations in the influent, (and consequently low solids loading rates), they ignored the coupling of the hydraulic and solids transport. This simplification can not be made for secondary clarifiers. Also, the authors' model was very sensitive to the initial conditions.

Imam and McCorquodale (1982) is another early attempt at modeling a neutral density flow inside a rectangular clarifier. Two coupled stream function-vorticity equations impose the equations of motion and continuity for the hydrodynamics in the clarifier. The ADI computational finite difference method is used to arrive at a solution. A variable size mesh is used which has more resolution in the inlet and outlet zones compared to the center region of the clarifier. The authors identify some of the shortcomings of their efforts; primarily that the eddy viscosity is assumed constant

throughout the tank. This was done to simplify the computations but is not a realistic assumption. Also, the effect of solids on the hydrodynamics is completely ignored.

Ostendorf (1986) provides an analytical solution of the turbulence and velocity fields for rectangular clarifiers. The author separates the clarifier into three different zones: the inlet zone, the settling zone, and the outlet or converging zone. The inlet, settling, and converging zones are characterized by turbulent jet, uniform, and converging flow fields. A Gaussian flow velocity profile is used for the turbulent jet zone. Downstream of the inlet zone, the settling zone is assumed to begin when the turbulent jet eddy reaches the clarifier surface. The author had less than 20% deviation between the velocity profile calculations and lab scale experiments. He concludes that the majority of the turbulence in a clarifier comes from the inlet jet rather than bottom and wall friction. Ostendorf notes the turbulence intensity in the inlet zone is about 10-20% of the mean flow velocity, which has the potential to resuspend sediment. While this type of analysis provides some meaningful insights about turbulence profiles in clarifiers, it can not describe the complicated hydrodynamic or solids flow patterns.

Stamou and Rodi (1989) report on the application of numerical computational methods for determining the two-dimensional flow field and solids concentration distribution inside a rectangular primary clarifier. It is assumed that there are no density effects because primary clarifiers receive influent solids concentrations near 150-200 mg/L. The hydrodynamics inside the clarifier are determined by solving five (5) coupled equations

with the TEACH numerical procedure developed by Gosman and Pun(1972). Three of the five equations impose the continuity and momentum conditions inside the clarifier. The other two solve the kappa-epsilon transport equations. The kappa-epsilon turbulence model predicts the kinematic viscosity in different regions in the clarifier. Prior to the kappa-epsilon turbulence model, it was always assumed that the kinematic viscosity distribution was constant, logarithmic, or parabolic. These prior assumptions did not accurately predict the kinematic viscosity distribution because the distribution depends on the flow velocity gradients in the clarifier. The flow pattern in a clarifier is complex, so the viscosity distribution cannot be accurately described as constant, logarithmic, or parabolic. After the flow distribution is determined, the suspended solids concentration distribution is calculated explicitly. The primary contribution of this paper is the successful use of the kappa-epsilon turbulence model.

Lyn and Rodi (1989) investigate the mean and turbulence characteristics of flow in the inlet region of a laboratory-scale rectangular settling tank. A plane jet was studied with different inlet baffle configurations. The author pointed out that the design of settling tanks is still empirical, despite the existence of several numerical models (Larsen 1977, Schamber *et al.* 1981, Imam *et al.* 1982, Stamou *et al.* 1989). There are few detailed measurements of the flow field characteristics of settling tanks available in the literature. For this reason, most of these numerical models have not been properly evaluated for their predictive ability. Some of Lyn and Rodi's conclusions are described below.

- Flow through curves are a poor way to determine the hydraulic efficiency of a settling tank with many baffles or a complex geometry.
- The three dimensional effects were stronger than expected by the authors.
- The turbulent transport (measured as a Reynolds stress) is maximum in the inlet zone, then declines quickly to a smaller value. The Reynolds stress measurements are significantly lower in the trials without the feedwell baffle.

Adams and Rodi (1990) present a numerical prediction of the flow field and suspended solids concentration distribution for a sedimentation tank. The numerical method uses the kappa-epsilon turbulence model, and a finite volume computational scheme. The paper repeats the experiments performed by Celik *et al.* (1985), using the same model equations, but with an improved numerical scheme. The purpose was to evaluate the effectiveness of the kappa-epsilon model with a computational scheme that minimizes numerical inaccuracies. Some conclusions from the investigation are listed below.

- The more complex the flow-field, the less accurate are the predictions. The flow patterns with one recirculation zone were predicted better than flow patterns with two or more recirculation zones.
- The kappa-epsilon's effectiveness lies in its ability to predict flow patterns without calibrating empirical constants.
- There are significant three-dimensional effects that are neglected in the present model.

Zhou and McCorquodale (1992a) present the first of a series of papers which are significantly different than many of the previous modeling efforts. The authors have developed a numerical model to predict the velocity and suspended solids concentration distribution for circular clarifiers. The model uses the SIMPLE (semi-implicit method

for pressure-linked equations) algorithm of Patankar and Spalding (1972) to solve for the incompressible hydraulic, sediment transport, and kappa-epsilon equations. The settling velocity used is a double exponential relationship suggested by Takacs and developed by Patry and Takacs (1992). There are a few features distinguishing this model from all previous attempts at numerical clarifier modeling. Some of the distinguishing features are listed below.

- This model is fully mass conservative. This improves the numerical stability of the simulation and provides more accurate results than non-mass conservative models.
- It is not assumed that the flow is neutrally buoyant. This is the first model to take density-driven effects into account. This is very important because for secondary clarifiers, density effects are significant. Most secondary clarifiers have a density waterfall, which were not predicted by earlier models.
- The slower settling solids are modeled more realistically with the double exponential settling equation.

Samstag *et al.* (1992) investigates the effects of the sludge withdrawal location on the effluent suspended solids concentration. Data from full scale testing was presented showing that when the RAS was withdrawn from the effluent end, or peripheral zone of circular secondary clarifiers, the ESS concentration was significantly lower (more than two-fold) than when the RAS was withdrawn from the influent end. A two-dimensional numerical model was also presented, and its results were compared to the field data. For the numerical model, the governing momentum and continuity equations for turbulent flow were transformed to a stream-vorticity transport equation, and the turbulent eddy viscosity transport was handled using a diffusion model proposed by Fischer *et al.*

(1979). The results from the numerical simulations were not in close agreement with the field data.

Wahlberg *et al.* (1994) examines the suspended solids settling characteristics as a function of the flocculation time. The authors found that for all the field data, the lowest background turbidity was obtained within ten minutes of flocculation. Additional flocculation time did not decrease the background turbidity. This suggests that a flocculation time for activated sludge processes of more than ten minutes is unnecessary.

The following papers all stem from the original effort of Zhou and McCorquodale (1991a).

- Zhou and McCorquodale (1992b)
- Zhou and McCorquodale (1992c)
- Zhou and McCorquodale (1992d)
- McCorquodale and Zhou (1993)
- Zhou, *et al.* (1994)
- Vitasovic, *et al.* (1997)

The main findings are summarized below.

- Circular Clarifiers have feedwell baffles around the influent zone. It was found that the optimal position depends on the dimensionless Froude number. If the feedwell baffle is too far, a density waterfall will develop, creating a recirculation eddy in the upper portion of the feedwell, and entraining fluid from the upper portion of the clarifier. If the

feedwell baffle is too close, a jet like condition develops, which creates a scouring effect on the sludge blanket.

- The authors have examined the effect of solids and hydraulic loading on clarifiers with and without feedwell baffles. This was analyzed using the dimensionless Froude number.
- The low Froude conditions correspond to the cases where the influent does not impinge strongly on the feedwell baffle. When the influent does not impinge on the baffle, its influent energy is not dissipated. This energy is then translated into kinetic energy as it travels down the wall, across the clarifier bottom, and up the wall on the effluent end, if strong enough.
- The greatest fluid entrainment occurs when the influent does not impinge on the baffle and falls straight down to the floor. As fluid is entrained, the bottom density current grows. In some cases, the flow rate of the bottom density current exceeds that of the influent flow.
- As the Froude number decreases, the upflow rate in the withdrawal zone increases. This has the effect of resuspending poorly settling solids, or not allowing them to settle at all.
- In general, the effluent suspended solids concentration is very sensitive to the withdrawal zone hydraulics.
- Increasing or decreasing the RAS ratio has significant effects on the clarifier. Because the influent flow is really the influent plant flow plus the RAS flow, increasing the RAS flow increases the inlet Froude number, which may improve or worsen the effluent quality.
- The relationship between the inlet Froude number and the effluent suspended solids concentration depends on the solids loading.
- Assuming a constant solids loading rate, the high hydraulic loading rate produces far better effluent quality than the low hydraulic loading rate scenario. (Zhou *et al.* 1993) This is due to the density waterfall generated in low hydraulic loading conditions. The density waterfall entrains fluid from the settling zone and has a significant effect on developing a recirculating flow pattern in the influent zone.
- The model agrees with most of the field data presented.

Zhong *et al.* (1996) presents a numerical model which couples the activated sludge aeration basin with the clarifier. The model uses a biological reaction structure developed by Clifft (1980) and Clifft and Andrews (1981). Stenstrom (1976) and Clifft (1980) compiled the kinetic rate equations and constants used. The clarifier sub model is

the same one developed by Zhou *et al.*(1991a). Simulations agreed closely with the field data presented.

Previous coupled models have been presented before (Stenstrom 1976, Vitasovic 1989, Dupont and Henze 1992). However, these models used a simplified clarifier submodel, which did not account for complex hydrodynamic flow patterns. The significance of this coupled model is that it can predict the dynamic solids inventory shifts that occur between an aeration basin and a clarifier while predicting the effluent suspended solids concentration leaving the clarifier with accuracy.

Wahlberg *et al.* (1997) is a discussion in response to the findings of Vitasovic *et al.* (1997). One of the main issues discussed are the limitations to modeling a clarifier without modeling the preceding aeration basin as well. The solids distribution between an aeration basin and a clarifier is a dynamic, closely coupled phenomenon. If a clarifier is overloaded with respect to thickening, much of the solids remain in the clarifier, and the RAS suspended solids concentration decreases. This would eventually lower the suspended solids concentration in the aeration basin, and the solids loading on the clarifier decreases, until the aeration tank and clarifier are in equilibrium. This is not reflected in the model used by Vitasovic *et al.* (1997). The authors also examined the effect the SOR and the SLR has on the ESS concentration. The overflow rate does not affect the ESS concentration until a critical overflow rate is reached. The ESS

concentration is far more dependent on the solids loading rate. As the solids loading rate increases, so does the ESS concentration.

CLARIFIER MODEL

The Reid Crowther Software Development Team in Seattle, Washington developed the two-dimensional clarifier model used for this thesis. The first version of this program was used, which models the hydraulic flow field and suspended solids concentration distribution for circular, center-feed clarifiers. Unlike some modeling programs, this program has a user-friendly interface in a windows-type format, which makes learning the program and maneuvering within it easy.

The input parameters needed for a simulation are listed and described below.

- Influent flow rate. The influent flow rate is defined as the flow rate through the clarifier at any given time. It is actually the flow entering the clarifier minus the return activated sludge flow rate. The influent flow rate can be held constant or varied over time.
- Mixed liquor concentration (influent suspended solids concentration). Like the influent flow rate, the mixed liquor concentration can be held constant or varied over time.
- Return activated sludge (RAS) flow rate or ratio. The return activated sludge can be withdrawn uniformly throughout the tank bottom, or at discrete radial positions along the tank bottom. The return activated sludge flow rate is chosen either as a discrete value, or a percentage of the influent flow rate. The RAS flow rate can not be varied over time in this version.
- Clarifier tank geometry. The dimensions needed to define the circular clarifier geometry is the radius, side water depth, floor bottom slope, baffle size and positions, and the influent well radius and depth.
- Suspended solids settling characteristics. The solids settling characteristics are defined by the Takacs *et al.* (1991) settling equation. The Takacs equation requires a Stokes single particle settling velocity, an empirical constant derived from settling batch data for the sludge to be used, and a calibration constant.

For each time step, the results given from a simulation are summarized below:

- The two-dimensional velocity field throughout the clarifier. The velocity field is provided in the radial and vertical direction. The program assumes that there is no angular component for simplicity
- The two-dimensional suspended solids concentration distribution.
- The mass of influent solids.
- The mass of solids returned to the aeration basin, and the RAS suspended solids concentration.

The last two items, the mass of influent solids and the mass of the returned solids are an important result for determining whether the simulation is near equilibrium. If the influent mass is significantly greater than the returned solids mass, this is an indication that the solids are not settling to the bottom quickly enough. When this is the case, the sludge blanket will rise in the clarifier until it flows over the effluent weirs, and the clarifier ultimately fails.

Mathematical Model

A detailed account of the computational methods used in this program is beyond the scope of this paper. A cursory account will be provided here. For a more detailed description of the model, Zhou *et al.* (1992c) provides a comprehensive account.

This clarifier model simulates the hydraulic and solids flow by using the finite-difference computational scheme of Patankar (1980). Essentially, the area inside the clarifier is discretized into a two-dimensional grid in the radial and vertical direction. There are 29 nodes in the radial dimension and 14 nodes in the vertical direction. To obtain more resolution where it is needed, variable grid spacing is used. Smaller grids are used near the water surface and in the effluent zone than in the rest of the clarifier.

All of the variables of concern are then solved at each grid point for each time step. Solving a series of coupled equations that approximate the differential equations describing the hydraulic and solids transport approximates the values at the grid points. These approximate equations are called finite-difference equations. What is unique about this program is that it is fully mass conservative. In other words, the influent mass flux equals the mass flux leaving through the effluent and return flow.

To provide a solution, the model solves the momentum, continuity, the kappa-epsilon turbulence equations, and the solids transport equations as a coupled system.

The Continuity Equation:

$$\frac{\partial ru}{\partial r}+\frac{\partial v}{\partial y}=0 \tag{5}$$

The Momentum Equation (radial direction):

$$\frac{\partial u}{\partial t}+u\frac{\partial u}{\partial r}+v\frac{\partial u}{\partial y}=-\frac{1}{\rho}\frac{\partial p}{\partial r}+\frac{1}{r}\frac{\partial}{\partial r}\left(r\upsilon_t\frac{\partial u}{\partial r}\right)+\frac{1}{r}\frac{\partial}{\partial y}\left(r\upsilon_t\frac{\partial u}{\partial y}\right)+S_u \tag{6}$$

The Momentum Equation (vertical direction):

$$\frac{\partial v}{\partial t}+u\frac{\partial v}{\partial r}v\frac{\partial v}{\partial y}=-\frac{1}{p}\frac{\partial p}{\partial y}+\frac{1}{r}\frac{\partial}{\partial r}\left(r\upsilon_t\frac{\partial v}{\partial r}\right)+\frac{1}{r}\frac{\partial}{\partial y}\left(r\upsilon_t\frac{\partial v}{\partial y}\right)-g\frac{\rho-\rho_r}{\rho}+S_v \quad (7)$$

Where,

r = radial co-ordinate

y = vertical co-ordinate

u = velocity in the radial direction

v = velocity in the vertical direction

p = pressure term

ρ = localized fluid density

ρ_r = density of clear water

υ_t = eddy viscosity

The terms S_u and S_v are defined as follows:

$$S_u=\frac{\partial}{\partial r}\left(r\upsilon_t\frac{\partial u}{\partial r}\right)+\frac{1}{r}\frac{\partial}{\partial y}\left(r\upsilon_t\frac{\partial v}{\partial t}\right)-2u\frac{\upsilon_t}{r^2} \quad (8)$$

$$S_v=\frac{\partial}{\partial r}\left(r\upsilon_t\frac{\partial u}{\partial y}\right)+\frac{1}{r}\frac{\partial}{\partial y}\left(r\upsilon_t\frac{\partial v}{\partial y}\right) \quad (9)$$

The Solids Transport Equations is as follows:

$$\frac{\partial C}{\partial t}+u\frac{\partial C}{\partial r}+v\frac{\partial C}{\partial y}=\frac{1}{r}\frac{\partial}{\partial r}\left(r\upsilon_{sr}\frac{\partial C}{\partial r}\right)+\frac{1}{r}\frac{\partial}{\partial y}\left(r\upsilon_{sy}\frac{\partial C}{\partial y}+rCV_s\right) \quad (10)$$

Where,

C = suspended solids concentration

V_s = particle settling velocity

υ_{sr} = eddy diffusivity for suspended solids in radial direction

υ_{sy} = eddy diffusivity for suspended solids in vertical direction

The suspended solids eddy diffusivity terms are related to the eddy viscosity and the empirical Schmidt number σ by the formula:

$$\upsilon_{sr} = \frac{\upsilon_t}{\sigma_{sr}} \tag{11}$$

$$\upsilon_{sy} = \frac{\upsilon_t}{\sigma_{sy}} \tag{12}$$

The eddy viscosity is calculated from the kappa-epsilon turbulence model. This turbulence model relates the eddy viscosity to the turbulent kinetic energy, κ, and the turbulent dissipation rate, ε. An empirical constant, C_μ is used for calibration.

$$\upsilon_t = C_\mu \frac{\kappa^2}{\varepsilon} \tag{13}$$

In the kappa-epsilon turbulence model, the distribution of kappa and epsilon will vary throughout the tank, depending on the velocity field distribution. The transport equations for kappa and epsilon are:

$$\frac{\partial \kappa}{\partial t} + u\frac{\partial \kappa}{\partial r} + v\frac{\partial \kappa}{\partial y} = \frac{1}{r}\frac{\partial}{\partial r}\left(r\frac{\upsilon_t}{\sigma_k}\frac{\partial \kappa}{\partial r}\right) + \frac{1}{r}\frac{\partial}{\partial y}\left(r\frac{\upsilon_t}{\sigma_k}\frac{\partial \kappa}{\partial y}\right) + P - \varepsilon \tag{14}$$

$$\frac{\partial \varepsilon}{\partial t} + u\frac{\partial \varepsilon}{\partial r} + v\frac{\partial \varepsilon}{\partial y} = \frac{1}{r}\frac{\partial}{\partial r}\left(r\frac{\upsilon_t}{\sigma_\varepsilon}\frac{\partial \varepsilon}{\partial r}\right) + \frac{1}{r}\frac{\partial}{\partial y}\left(r\frac{\upsilon_t}{\sigma_\varepsilon}\frac{\partial \varepsilon}{\partial y}\right) + C_1 P\frac{\varepsilon}{\kappa} - C_2\frac{\varepsilon^2}{\kappa} \tag{15}$$

The constants C_1, C_2, σ_κ, and σ_ε are chosen from empirical data. The variable P is the turbulent energy production and is defined as:

$$P = \upsilon_t\left[2\left(\frac{\partial u}{\partial r}\right)^2 + 2\left(\frac{\partial v}{\partial r}\right)^2 + 2\left(\frac{u}{r}\right)^2 + \left(\frac{\partial u}{\partial y} + \frac{\partial v}{\partial r}\right)^2\right] \tag{16}$$

The settling model used is the settling equation by Takacs *et al.* (1991) and Patry *et al.*. (1992). It is as follows:

$$V_s = V_0\left[e^{-K_1(C-C_{min})} - e^{-K_2(C-C_{min})}\right] \tag{17}$$

Where,

V_s = actual settling velocity

V_0 = Stokes particle settling velocity

K_1 = empirical constant describing settling velocity of rapidly settling particles

K_2 = empirical constant describing settling velocity of poorly settling particles

C = localized suspended solids concentration

C_{min} = concentration of non-settleable particles

In this version of the program, C_{min} was fixed at 0.2% of the influent suspended solids concentration.

The boundary conditions imposed on the solution set are:

- all boundaries have zero velocity components in the radial and vertical direction at all times;
- the baffles were treated as reflecting boundaries; and
- the log-law is used to determine the fluid velocities in near-wall regions.

The initial conditions are:

- the velocities and suspended solids concentrations are zero at all grid points;
- a constant is initially assigned to all kappa and epsilon values throughout the clarifier; and
- there are no solids in the clarifier; solids begin entering the clarifier through the inlet zone when the simulation begins.

SIMULATIONS

A total of one hundred and thirteen simulations were performed. The simulations were arranged into seven sets and described in matrices. By varying the influent flow rate, the return solids flow rate, the mixed liquor suspended solids concentration, and sometimes the clarifier geometry, observations were made to identify the effects the following process variables have on the effluent suspended solids concentration:

- surface overflow rate SOR;
- solids loading rate (SLR);
- clarifier hydraulics; and
- clarifier geometry (side water depth and feed well skirt depth).

Matrix 1 included 16 simulations and was the first set of simulations performed. These simulations formed the basis for the rest of the paper. All parameters were kept constant throughout the simulations except for the influent flow rate and the return solids flow rate. Four solids loading rates were used, 2.04, 3.06, 4.08, and 5.10 $kg/m^2/hr$. For each solids loading rate four simulations were performed with different combinations of influent flow and return activated sludge to give equal solids loading rates.

Matrix 2 included 8 simulations. Two different surface overflow rates were used, 0.46 and 1.14 m/hr. For each surface overflow rate, four simulations were performed with

different solids loading rates. As in matrix 1, different combinations of influent flow and return activated sludge flow were used to give equal surface overflow rates while varying the solids loading rates. All other parameters remained constant.

Matrix 3 was comprised of 16 simulations. However, in addition to varying the influent and RAS flow rate, the mixed liquor suspended solids (MLSS) concentration was varied as well. The same four solids loading rates used in matrix 1 were used here as well. The RAS flow rate was maintained at 50% of the influent flow rate. For each solids loading rate, the influent flow was increased as the mixed liquor concentration was decreased to maintain the same solids loading rate. All other input parameters remained constant. However, because the influent mixed liquor concentration was varied, the single particle settling velocity did not remain constant.

Matrices 4, 5, and 6 are exactly the same as matrix 1, except the clarifier side water depth and baffle depth is varied. In matrix 4, the side water depth is 10 m (more than twice as deep as in matrix 1-3) and the feed well skirt depth is 5.9 m. In matrix 5, the side water depth is 10 m again while the feed well skirt depth is the same as that used for matrix 1, 2.44 m. In matrix 6, the side water depth is 10 m, and there is no feed well skirt.

Matrix 7 was performed for a sensitivity analysis. Five scenarios were chosen, and each scenario was run with five different time steps used for the computations.

Input Parameters

Many of the input parameters are shown in tables 2-8 with the results. All of the input parameters for each simulation were kept constant throughout the duration of the simulation. The influent flow rate, the RAS flow rate, and the mixed liquor concentration parameters are self-explanatory. Below are brief explanations of the other input parameters and conditions used for the simulations.

Time Step

The modeling program computes the fluid velocity and suspended solids concentration at each grid point for each time step as it marches toward a solution. A three-minute time step is the default value for this program and has been shown to work adequately. Choosing too large of a time step may cause computational instability, and choosing too small of a time step may cause numerical instability. Numerical instability arises when the errors due to approximations made at every time step cause the solution to diverge and give a result that may be "unreal."

Duration of Simulation

All simulations were modeled for 600 minutes, or 10 hours. It is assumed that a clarifier that will not fail will reach equilibrium within this time.

Suspended Solids Settling Characteristics

The following parameters were used for the solids settling characteristics for each simulation:

- a Stokes settling velocity of 11.1 m/hr;
- K_1 was set at 0.607 Liters/gram; and
- K_2 was set at 0.1.

Clarifier Geometry

Four different clarifier geometries were used for the simulations. The clarifier geometry used for simulations in matrix 1, 2, 3, and most of 7 are taken from studies performed by Wahlberg *et al.* (1994) and Vitasovic *et al.* (1997). This is noted as geometry A in the result table. Geometry B is the same as A, except for a deeper side water depth and feed well skirt. Geometry C is the same as B, except for a deeper side water depth. Finally, geometry D is the same as B and C, except there is no feed well skirt. The surface area of all four geometries is 1428 m^2. The geometries are tabulated in table 1.

TABLE 1.

Geometric Input Parameters

Geometry	Side Wall Radius (m)	Side Wall Depth (m)	Feed Well Inlet Radius (m)	Feed Well Inlet Depth (m)	Feed Well Skirt Depth (m)	Feed Well Skirt Radius (m)	Bottom Slope (%)
A	21.34	4.36	0.9	1.0	2.44	9.76	2.0
B	21.34	10.0	0.9	1.0	5.9	9.76	2.0
C	21.34	10.0	0.9	1.0	2.44	9.76	2.0
D	21.34	10.0	0.9	1.0	0.0	N/A	2.0

The dimensions in table 1 are illustrated below in figure 1.

FIGURE 1.

CLARIFIER GEOMETRY INPUT PARAMETERS

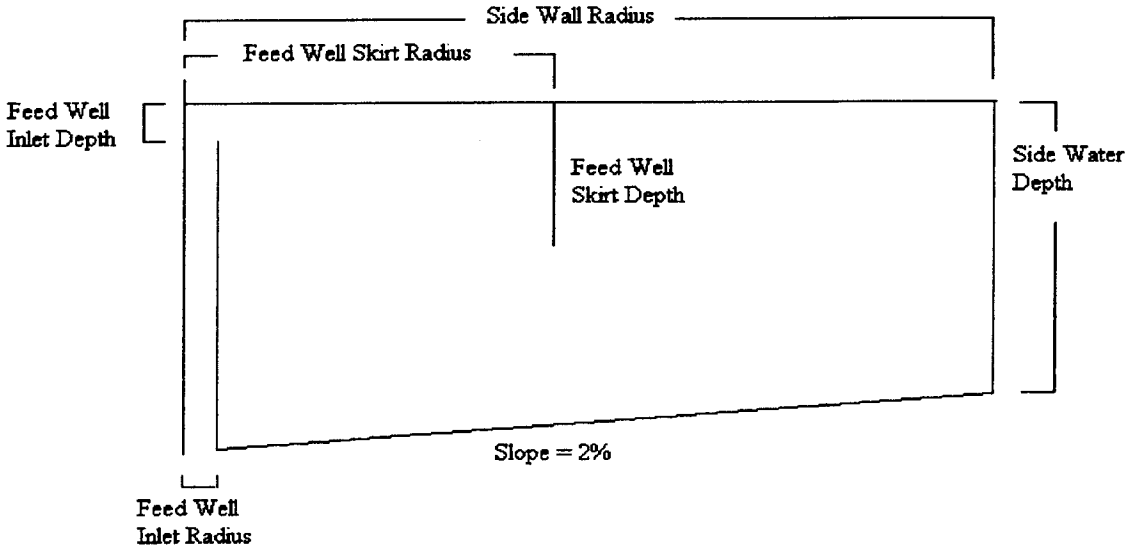

Return Activated Solids Flow Rate Geometry

The return solids were withdrawn from the bottom of the tank uniformly. This is a simplification of how solids are actually withdrawn from clarifiers. Most sludge withdrawal mechanisms withdraw sludge with riser pipes which rotate along the bottom and withdraw sludge from specific radial positions, or are scraped towards the center and withdrawn from there. Even though the program allows sludge to be withdrawn from specific locations along the bottom, which represents the riser pipes configuration well, the author assumed that results obtained with a uniform withdrawal would not deviate too far from reality. Newer versions of this program have incorporated scraper withdrawal mechanisms.

RESULTS

The results of all the simulations are tabulated below in tables 2-8 and graphed in figures 2-9. The bold entries in tables 2-8 are those simulations that failed, or did not reach equilibrium within 600 minutes of simulation time.

As mentioned earlier, all the simulations were run for a ten hour period. The simulations which performed well reached equilibrium within two to three hours. When the ESS concentration did not reach equilibrium after ten hours, those simulations were considered as failed runs. When looking at the suspended solids concentration distribution for the entire clarifier, it was clear that the sludge blanket level was rising for those simulations that were failed.

Some of these simulations were run until an effluent solids concentration equilibrium was reached near 500-600 mg/L. These simulation results were still included in tables 2-8, yet it is also noted that they did not reach equilibrium after ten hours, so they were not included in any of the graphs in figures 2-9.

In Appendix A, the velocity profile and the suspended solids concentration distribution is displayed at 600 minutes for simulations 1-88. Appendix A also contains the ESS concentration as a function of time for all 88 simulations.

Appendix B contains the velocity profiles and suspended solids concentration distribution of simulation 12 at different times to illustrate the progression of the rising sludge blanket level, and the clarifier's ultimate failure.

Matrix 1

Simulations were performed for four different SOR's for each of the four different solids loading rates. Although there was a slight increase in the ESS concentration as the SOR increased, there was a greater dependence on the solids loading rate. The plot suggests in fact, that the SOR does not influence the ESS concentration strongly, until a critical SOR threshold is reached. For three of the four solids loading rates, the ESS remains relatively constant, then increases after the SOR is beyond approximately 1 m/hr. It is difficult to identify a specific threshold, but it does seem to depend on the solids loading rate. As the solids loading rate increases, it appears that the ESS concentration increases at a lower SOR. These results agree with Wahlberg *et al.* (1993) in their conclusion that "no relationship between ESS and SOR could be shown..." within the tested range of 0.5-1.5 m/hr. Six of the sixteen simulations (simulation 4, 8, 11, 12, 14, & 15) in this matrix failed, or did not reach equilibrium in ten hours. These simulations were those with the highest surface overflow rates for each solids loading rate. This is a clear case of how the hydraulics in the clarifier has impaired the solids settling and the clarification of the flow.

TABLE 2.

Simulation Matrix 1 Results

Run No.	Time Step (min)	Clarifier Geometry (A, B, C, D)	Influent Flow (m^3/hr)	MLSS (mg/L)	Ras Flow (m^3/hr)	Ras/ Influent	SOR (m/hr)	SLR (kg/m^2/hr)	ESS (mg/L)	Equilib-rium?
1	3	A	503	2363	729	1.45	0.35	2.04	6.47	Yes
2	3	A	746	2363	486	0.65	0.52	2.04	6.72	Yes
3	3	A	869	2363	364	0.42	0.61	2.04	6.65	Yes
4	**3**	**A**	**914**	**2363**	**317**	**0.35**	**0.64**	**2.04**	**6.57**	**No**
5	3	A	757	2363	1092	1.44	0.53	3.06	7.73	Yes
6	3	A	1120	2363	729	0.65	0.78	3.06	8.14	Yes
7	3	A	1303	2363	546	0.42	0.91	3.06	7.76	Yes
8	**3**	**A**	**1412**	**2363**	**439**	**0.31**	**0.99**	**3.06**	**11.30**	**No**
9	3	A	524	2363	1942	3.71	0.37	4.08	8.92	Yes
10	3	A	1301	2363	1164	0.89	0.91	4.08	10.40	Yes
11	**3**	**A**	**1634**	**2363**	**831**	**0.51**	**1.14**	**4.08**	**10.40**	**No**
12	**3**	**A**	**1819**	**2363**	**647**	**0.36**	**1.27**	**4.08**	**11.70**	**No**
13	3	A	655	2363	2428	3.71	0.46	5.10	11.90	Yes
14	3	A	1626	2363	1456	0.90	1.14	5.10	14.50	Yes
15	**3**	**A**	**2043**	**2363**	**1039**	0.51	**1.43**	**5.10**	**22.60**	**No**
16	**3**	**A**	**2241**	**2363**	**841**	**0.38**	**1.57**	**5.10**	**117.00**	**No**

FIGURE 2.

Simulation Matrix 1

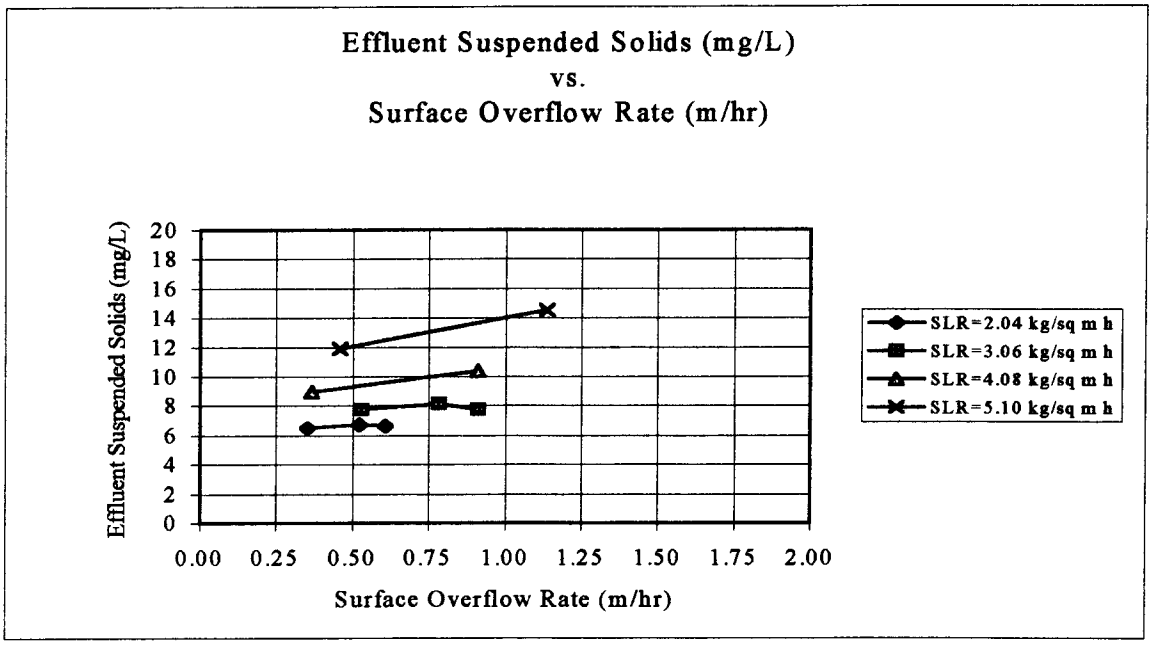

Matrix 2

Matrix 2 includes a total of eight simulations at two different surface overflow rates. For each surface overflow rate, there is a range of simulated solids loading rates. Figure 3 shows the effluent suspended solids concentration versus the solids loading rate and shows a very strong correlation between the two. This graph suggests that increasing the solids loading rate will increase the ESS concentration, and that the surface overflow rate is not a significant parameter within the tested range. In fact, the curves of the two different surface overflow rates lay directly on top of each other. This agrees well with the results in matrix 1. In matrix 1, the effluent suspended solids concentration was not affected significantly by the surface overflow rate until it was greater than 1.0 meters/hour. The two surface overflow rates used in matrix 2 were 0.46 and 1.14 m/hr, which is not much greater than 1.0 m/hr. Only one of the eight simulations failed since relatively low surface overflow rates were used. Interestingly, the simulation with the highest solids loading rate modeled in this thesis was in this matrix, and reached equilibrium within a few hours. The simulation that failed did not have a particularly high surface overflow rate or solids loading rate.

TABLE 3.

Simulation Matrix 2 Results

Run No.	Time Step (min)	Clarifier Geometry (A, B, C, D)	Influent Flow (m^3/hr)	MLSS (mg/L)	Ras Flow (m^3/hr)	Ras/ Influent	SOR (m/hr)	SLR (kg/m^2/hr)	ESS (mg/L)	Equilib-rium?
17	3	A	655	2363	158	0.24	0.46	1.35	6.09	Yes
18	3	A	655	2363	584	0.89	0.46	2.05	6.58	Yes
19	3	A	655	2363	1262	1.93	0.46	3.17	7.64	Yes
20	3	A	655	2363	2366	3.61	0.46	5.00	11.60	Yes
21	**3**	**A**	**1626**	**2363**	**536**	**0.33**	**1.14**	**3.58**	**9.80**	**No**
22	3	A	1626	2363	631	0.39	1.14	3.73	9.58	Yes
23	3	A	1626	2363	1262	0.78	1.14	4.78	13.20	Yes
24	3	A	1626	2363	1940	1.19	1.14	5.90	18.50	Yes

FIGURE 3.

Simulation Matrix 2

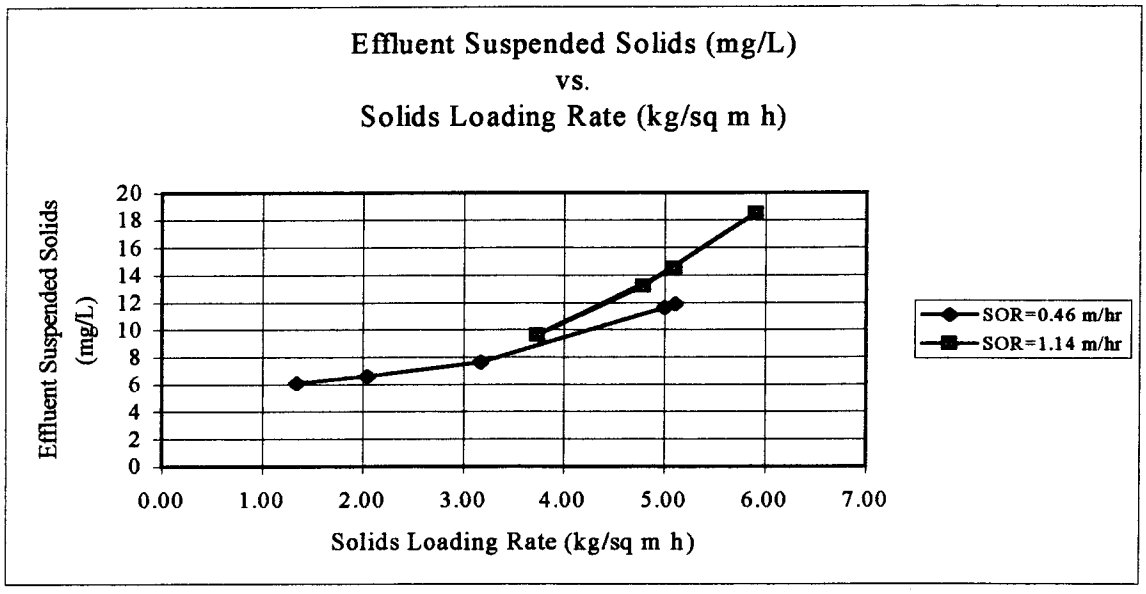

Matrix 3

Matrix 3 contains sixteen simulations for the same four solids loading rates used in matrix 1. The main difference between matrix three and matrix 1 is that a constant solids loading rate was achieved by varying the mixed liquor concentration as well as the influent flow and RAS flow. Half of the simulations in this matrix did not reach equilibrium, and consequently failed. The simulations that failed were not those that were hydraulically overloaded with respect to the SOR, nor those that were overloaded with respect to the SOR or SLR, but those with a high influent suspended solids concentration. Seven of the eight failing simulations had surface overflow rates and solids loading rates well within the range used for previous simulations which easily reached equilibrium. It appears that the main factor that caused these simulations to fail was the high influent solids concentration (3,000 mg/L and 4,000 mg/L). As the influent solids concentration increases, the SVI, or sludge volume index increases, which reduces the effective single particle settling velocity. For identical solids loadings, the simulations with high influent solids concentrations developed a thick sludge blanket very quickly compared to those simulations with a lower influent solids concentration.

TABLE 4.

Simulation Matrix 3 Results

Run No.	Time Step (min)	Clarifier Geometry (A, B, C, D)	Influent Flow (m^3/hr)	MLSS (mg/L)	Ras Flow (m^3/hr)	Ras/ Influent	SOR (m/hr)	SLR (kg/m^2/hr)	ESS (mg/L)	Equilib-rium?
25	3	A	1972	1000	971	0.50	1.36	2.04	12.30	Yes
26	3	A	971	2000	486	0.50	0.68	2.04	6.79	Yes
27	3	A	647	3000	324	0.50	0.45	2.04	6.65	Yes
28	**3**	**A**	**486**	**4000**	**243**	**0.50**	**0.34**	**2.04**	**7.16**	**No**
29	3	A	2914	1000	1457	0.50	2.04	3.06	39.00	Yes
30	3	A	1456	2000	728	0.50	1.02	3.06	9.03	Yes
31	**3**	**A**	**971**	**3000**	**486**	**0.50**	**0.68**	**3.06**	**7.83**	**No**
32	**3**	**A**	**728**	**4000**	**364**	**0.50**	**0.51**	**3.06**	**12.30**	**No**
33	3	A	3885	1000	1942	0.50	2.72	4.08	109.00	Yes
34	3	A	1942	2000	971	0.50	1.36	4.08	14.10	Yes
35	**3**	**A**	**1295**	**3000**	**648**	**0.50**	**0.91**	**4.08**	**9.62**	**No**
36	**3**	**A**	**971**	**4000**	**485**	**0.50**	**0.68**	**4.08**	**30.80**	**No**
37	3	A	4856	1000	2428	0.50	3.40	5.10	224.00	Yes
38	**3**	**A**	**2428**	**2000**	**1214**	**0.50**	**1.70**	**5.10**	**36.10**	**No**
39	**3**	**A**	**1618**	**3000**	**810**	**0.50**	**1.13**	**5.10**	**29.70**	**No**
40	**3**	**A**	**1214**	**4000**	**607**	**0.50**	**0.85**	**5.10**	**188.00**	**No**

Matrix 4

Sixteen simulations were performed for matrix four, which were identical to matrix 1 except that the side water depth was increased along with the feed well skirt depth. The results are plotted in figure 4. The results showed almost negligible dependence of the effluent suspended solids concentration on the surface overflow rate within the entire range tested of 0.35 to 1.57 m/hr. Also, the effluent solids concentration did not show a dependence on the solids loading rate until the high loading of 5.10 $kg/m^2/hr$ was used. The effluent suspended solids concentration was slightly higher than the results from matrix 1, where the shallower clarifier was used. Three of the 16 simulations failed due to a rising sludge blanket. Even though the effluent suspended solids was actually higher than that for the shallower clarifier, these results suggest that the deeper clarifier can handle a higher hydraulic load (influent flow + RAS flow) than shallower clarifiers.

TABLE 5.

Simulation Matrix 4 Results

Run No.	Time Step (min)	Clarifier Geometry (A, B, C, D)	Influent Flow (m^3/hr)	MLSS (mg/L)	Ras Flow (m^3/hr)	Ras/ Influent	SOR (m/hr)	SLR (kg/m^2/hr)	ESS (mg/L)	Equilib-Rium?
41	3	B	503	2363	729	1.45	0.35	2.04	8.54	Yes
42	3	B	746	2363	486	0.65	0.52	2.04	8.71	Yes
43	3	B	869	2363	364	0.42	0.61	2.04	8.63	Yes
44	3	B	914	2363	317	0.35	0.64	2.04	8.60	Yes
45	3	B	757	2363	1092	1.44	0.53	3.06	7.85	Yes
46	3	B	1120	2363	729	0.65	0.78	3.06	8.03	Yes
47	3	B	1303	2363	546	0.42	0.91	3.06	8.06	Yes
48	**3**	**B**	**1412**	**2363**	**439**	**0.31**	**0.99**	**3.06**	**7.99**	**No**
49	3	B	524	2363	1942	3.71	0.37	4.08	7.79	Yes
50	3	B	1301	2363	1164	0.89	0.91	4.08	8.47	Yes
51	3	B	1634	2363	831	0.51	1.14	4.08	9.35	Yes
52	**3**	**B**	**1819**	**2363**	**647**	**0.36**	**1.27**	**4.08**	**8.92**	**No**
53	3	B	655	2363	2428	3.71	0.46	5.10	12.20	Yes
54	3	B	1626	2363	1456	0.90	1.14	5.10	14.70	Yes
55	3	B	2043	2363	1039	0.51	1.43	5.10	15.00	Yes
56	**3**	**B**	**2241**	**2363**	**841**	**0.38**	**1.57**	**5.10**	**14.40**	**No**

FIGURE 4.

Simulation Matrix 4

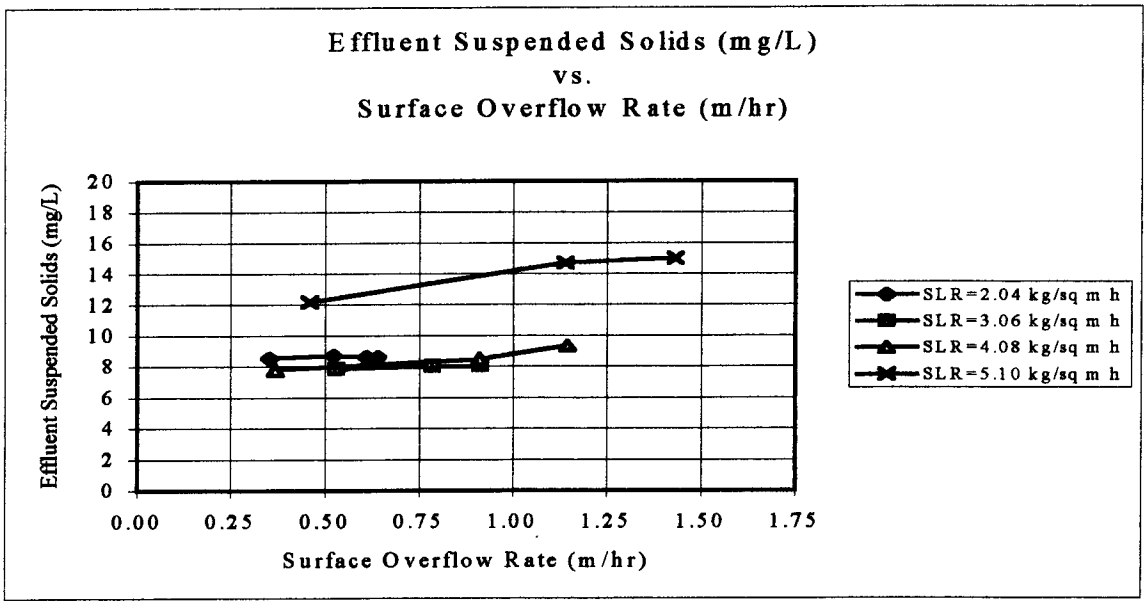

Matrix 5

Sixteen simulations were performed for matrix five, which were identical to matrix 4, except that a shorter feed well skirt depth was used, the same depth used in matrix 1, 2.44 meters. Except for the simulations with a solids loading rate of 2.04 $kg/m^2/hr$, the effluent suspended solids correlated strongly with the surface overflow rate, and not the solids loading rate, as observed in matrix one, two, and four. Interestingly, the two simulations that reached equilibrium with the lowest solids loading rate of 2.04 $kg/m^2/hr$ produced the highest effluent suspended solids concentrations in the entire matrix.

Matrix 6

Sixteen simulations were performed for matrix six. The input parameters were similar to matrices four and five, except there was no feed well skirt. The results from the simulations in this matrix were practically identical to those of matrix five.

TABLE 6.

Simulation Matrix 5 Results

Run No.	Time Step (min)	Clarifier Geometry (A, B, C, D)	Influent Flow (m^3/hr)	MLSS (mg/L)	Ras Flow (m^3/hr)	Ras/ Influent	SOR (m/hr)	SLR (kg/m^2/hr)	ESS (mg/L)	Equilib-Rium?
57	3	C	503	2363	729	1.45	0.35	2.04	12.30	Yes
58	3	C	746	2363	486	0.65	0.52	2.04	13.50	Yes
59	**3**	**C**	**869**	**2363**	**364**	**0.42**	**0.61**	**2.04**	**13.80**	**No**
60	**3**	**C**	**914**	**2363**	**317**	**0.35**	**0.64**	**2.04**	**13.90**	**No**
61	3	C	757	2363	1092	1.44	0.53	3.06	7.24	Yes
62	3	C	1120	2363	729	0.65	0.78	3.06	7.44	Yes
63	3	C	1303	2363	546	0.42	0.91	3.06	8.15	Yes
64	**3**	**C**	**1412**	**2363**	**439**	**0.31**	**0.99**	**3.06**	**10.20**	**No**
65	3	C	524	2363	1942	3.71	0.37	4.08	6.91	Yes
66	3	C	1301	2363	1164	0.89	0.91	4.08	7.92	Yes
67	3	C	1634	2363	831	0.51	1.14	4.08	9.67	Yes
68	3	C	1819	2363	647	0.36	1.27	4.08	11.50	Yes
69	3	C	655	2363	2428	3.71	0.46	5.10	7.66	Yes
70	3	C	1626	2363	1456	0.90	1.14	5.10	10.40	Yes
71	3	C	2043	2363	1039	0.51	1.43	5.10	13.00	Yes
72	3	C	2241	2363	841	0.38	1.57	5.10	16.50	Yes

FIGURE 5.

Simulation Matrix 5

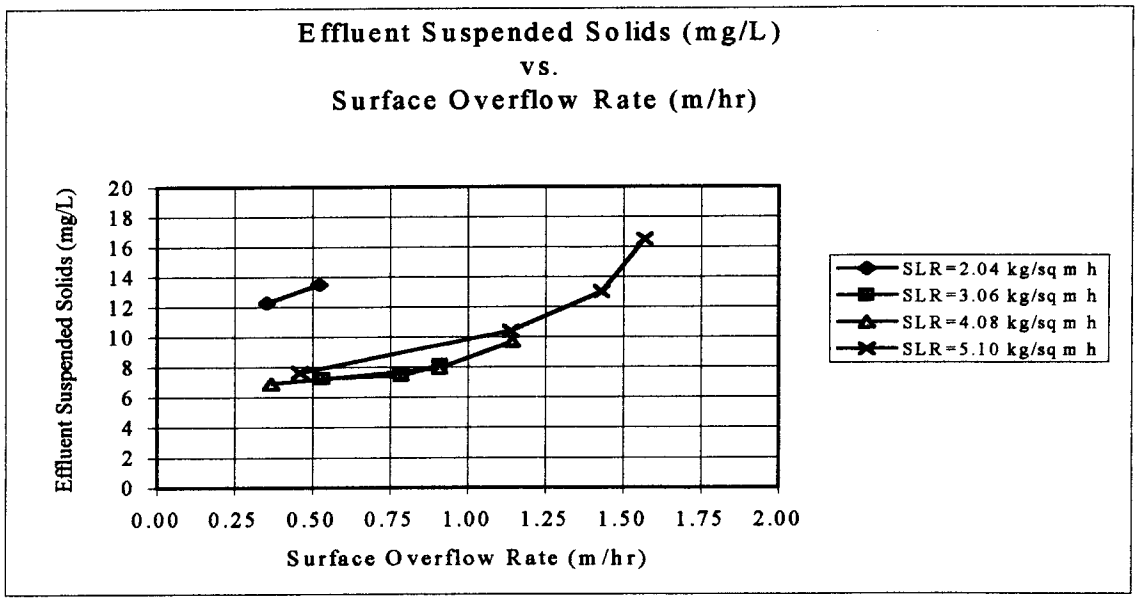

TABLE 7.

Simulation Matrix 6 Results

Run No.	Time Step (min)	Clarifier Geometry (A, B, C, D)	Influent Flow (m^3/hr)	MLSS (mg/L)	Ras Flow (m^3/hr)	Ras/ Influent	SOR (m/hr)	SLR (kg/m^2/hr)	ESS (mg/L)	Equilib-Rium?
73	3	D	503	2363	729	1.45	0.35	2.04	12.20	Yes
74	3	D	746	2363	486	0.65	0.52	2.04	13.80	Yes
75	3	D	869	2363	364	0.42	0.61	2.04	14.20	Yes
76	**3**	**D**	**914**	**2363**	**317**	**0.35**	**0.64**	**2.04**	**14.30**	**No**
77	3	D	757	2363	1092	1.44	0.53	3.06	7.02	Yes
78	3	D	1120	2363	729	0.65	0.78	3.06	7.29	Yes
79	3	D	1303	2363	546	0.42	0.91	3.06	7.96	Yes
80	**3**	**D**	**1412**	**2363**	**439**	**0.31**	**0.99**	**3.06**	**8.02**	**No**
81	3	D	524	2363	1942	3.71	0.37	4.08	6.79	Yes
82	3	D	1301	2363	1164	0.89	0.91	4.08	7.56	Yes
83	3	D	1634	2363	831	0.51	1.14	4.08	9.46	Yes
84	**3**	**D**	**1819**	**2363**	**647**	**0.36**	**1.27**	**4.08**	**12.10**	**No**
85	3	D	655	2363	2428	3.71	0.46	5.10	7.61	Yes
86	3	D	1626	2363	1456	0.90	1.14	5.10	10.30	Yes
87	3	D	2043	2363	1039	0.51	1.43	5.10	12.90	Yes
88	3	D	2241	2363	841	0.38	1.57	5.10	15.70	Yes

FIGURE 6.

Simulation Matrix 6

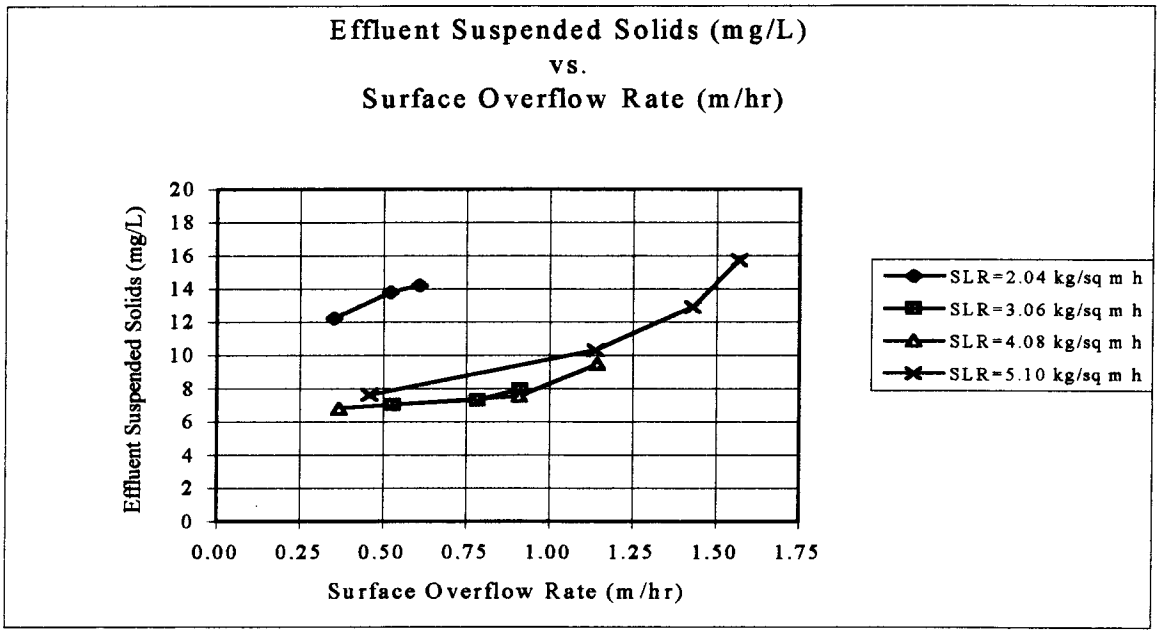

Matrix 7

Twenty-five simulations were performed for matrix 7 as a sensitivity analysis of the program to the time step used for its calculations. Five previously performed simulations were chosen, three of which reached equilibrium and produced desirable ESS concentrations, while the other two were unstable and did not reach equilibrium within the simulation time. Each simulation was run for time steps ranging from one to four minutes. There was no significant effect on the equilibrium ESS concentration as the time step was varied from one to four minutes. For the simulations that previously failed, they still failed. However, it seemed that by decreasing the time step, the increasing sludge blanket levels would rise more slowly. Nevertheless, equilibrium results of this program in terms of ESS concentration were not very sensitive to the time step used.

TABLE 8.

Simulation Matrix 7 Results

Run No.	Time Step (min)	Clarifier Geometry (A, B, C, D)	Influent Flow (m^3/hr)	MLSS (mg/L)	Ras Flow (m^3/hr)	Ras/ Influent	SOR (m/hr)	SLR (kg/m^2/hr)	ESS (mg/L)	Equilib-Rium?
89	1	A	1303	2363	546	0.42	0.91	3.06	7.76	Yes
90	2	A	1303	2363	546	0.42	0.91	3.06	7.76	Yes
91	2.5	A	1303	2363	546	0.42	0.91	3.06	7.78	Yes
92	3	A	1303	2363	546	0.42	0.91	3.06	7.76	Yes
93	4	A	1303	2363	546	0.42	0.91	3.06	7.74	Yes
94	1	**A**	**1412**	**2363**	**439**	**0.31**	**0.99**	**3.06**	**8.81**	**No**
95	2	**A**	**1412**	**2363**	**439**	**0.31**	**0.99**	**3.06**	**8.94**	**No**
96	2.5	**A**	**1412**	**2363**	**439**	**0.31**	**0.99**	**3.06**	**8.99**	**No**
97	3	**A**	**1412**	**2363**	**439**	**0.31**	**0.99**	**3.06**	**11.30**	**No**
98	4	**A**	**1412**	**2363**	**439**	**0.31**	**0.99**	**3.06**	**18.90**	**No**
99	1	A	655	2363	2366	3.61	0.46	5.00	11.80	Yes
100	2	A	655	2363	2366	3.61	0.46	5.00	11.60	Yes
101	2.5	A	655	2363	2366	3.61	0.46	5.00	11.60	Yes
102	3	A	655	2363	2366	3.61	0.46	5.00	11.60	Yes
103	4	A	655	2363	2366	3.61	0.46	5.00	11.70	Yes
104	1	**A**	**1626**	**2363**	**536**	**0.33**	**1.14**	**3.58**	**9.10**	**No**
105	2	**A**	**1626**	**2363**	**536**	**0.33**	**1.14**	**3.58**	**9.08**	**No**
106	2.5	**A**	**1626**	**2363**	**536**	**0.33**	**1.14**	**3.58**	**10.90**	**No**
107	3	**A**	**1626**	**2363**	**536**	**0.33**	**1.14**	**3.58**	**9.80**	**No**
108	4	**A**	**1626**	**2363**	**536**	**0.33**	**1.14**	**3.58**	**32.80**	**No**
109	1	D	2241	2363	841	0.38	1.57	5.10	15.70	Yes
110	2	D	2241	2363	841	0.38	1.57	5.10	15.70	Yes
111	2.5	D	2241	2363	841	0.38	1.57	5.10	15.70	Yes
112	3	D	2241	2363	841	0.38	1.57	5.10	15.70	Yes
113	4	D	2241	2363	841	0.38	1.57	5.10	15.70	Yes

FIGURE 7.

Simulation Matrix 7

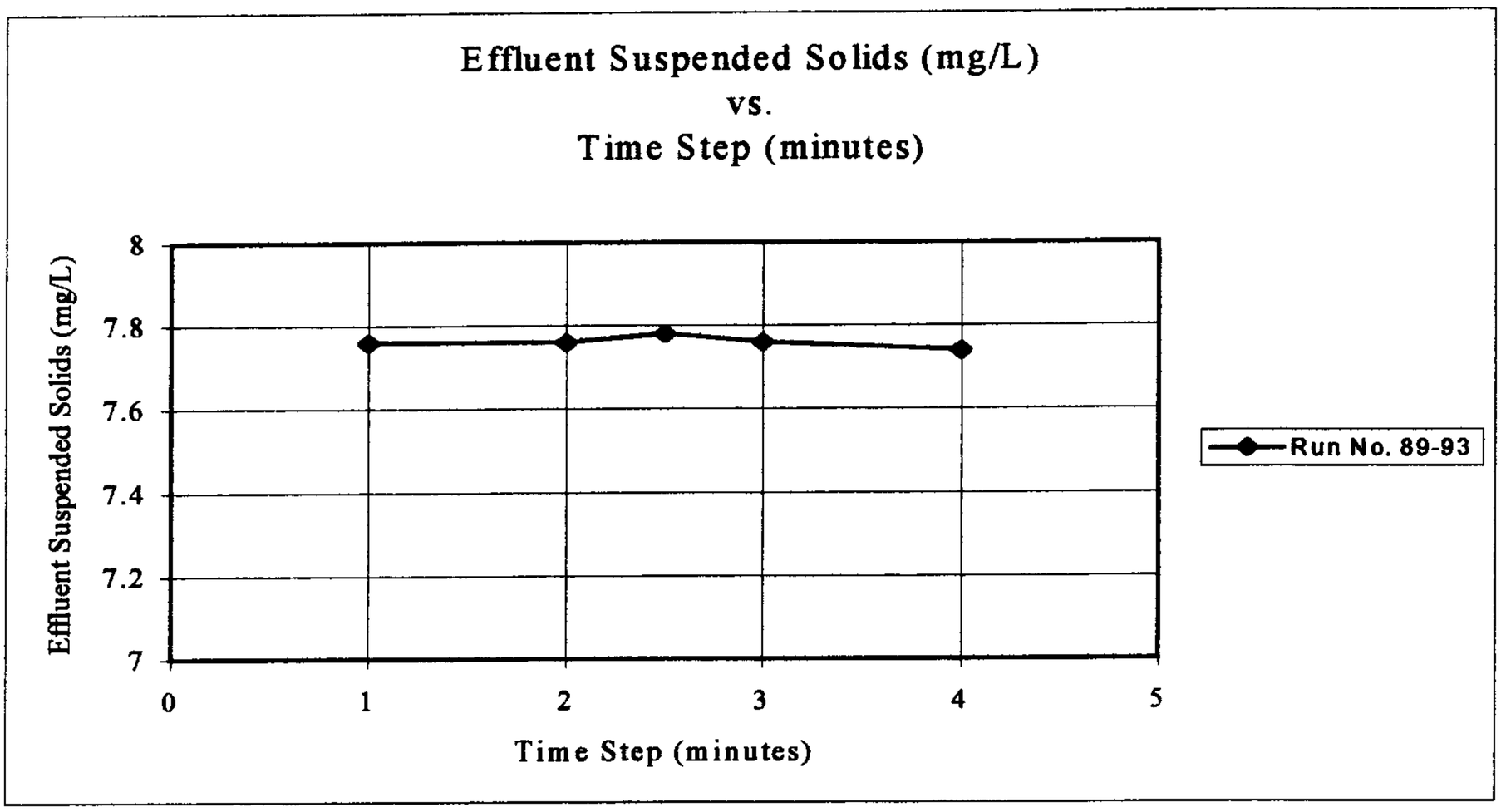

FIGURE 8.

Simulation Matrix 7

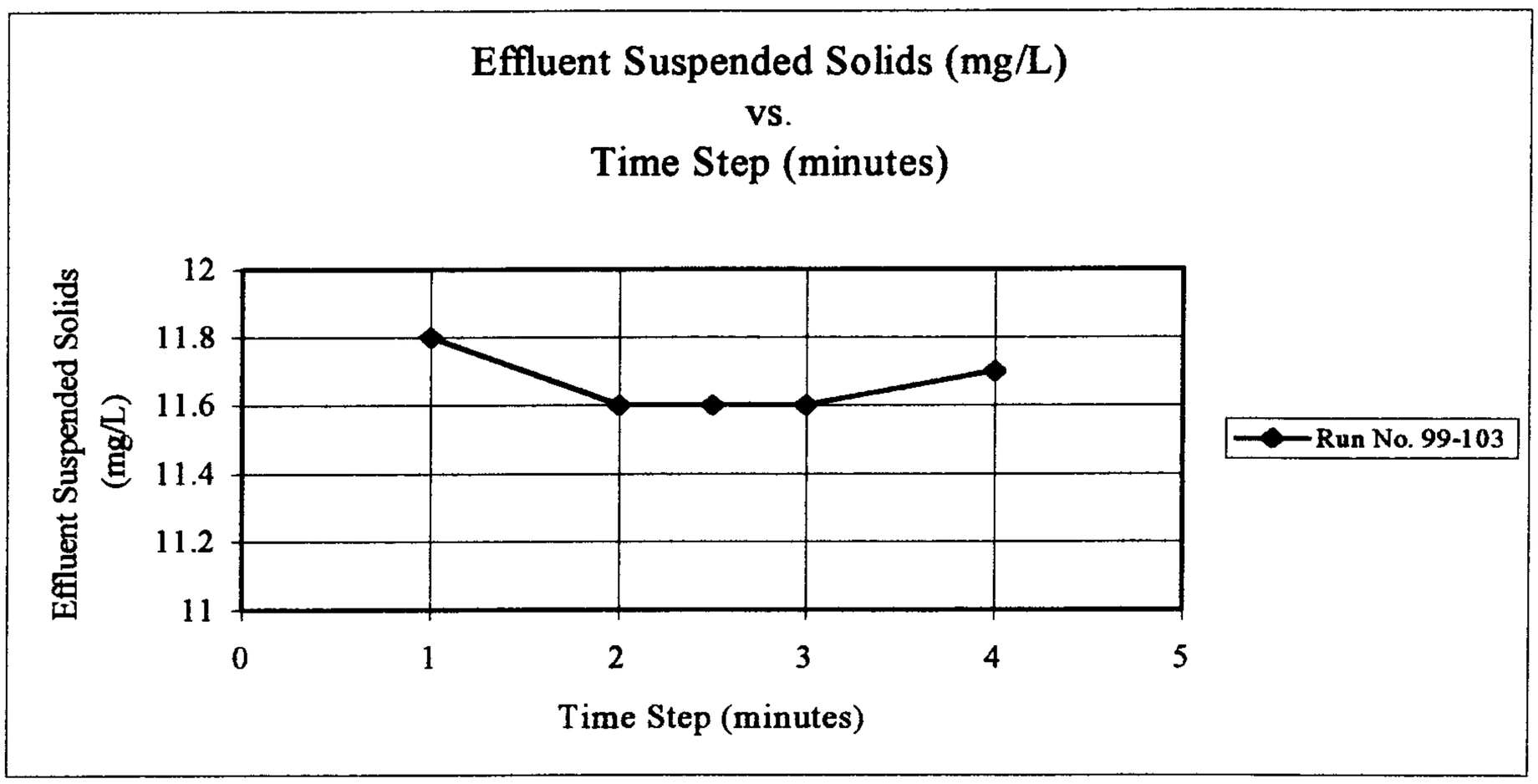

FIGURE 9.

Simulation Matrix 7

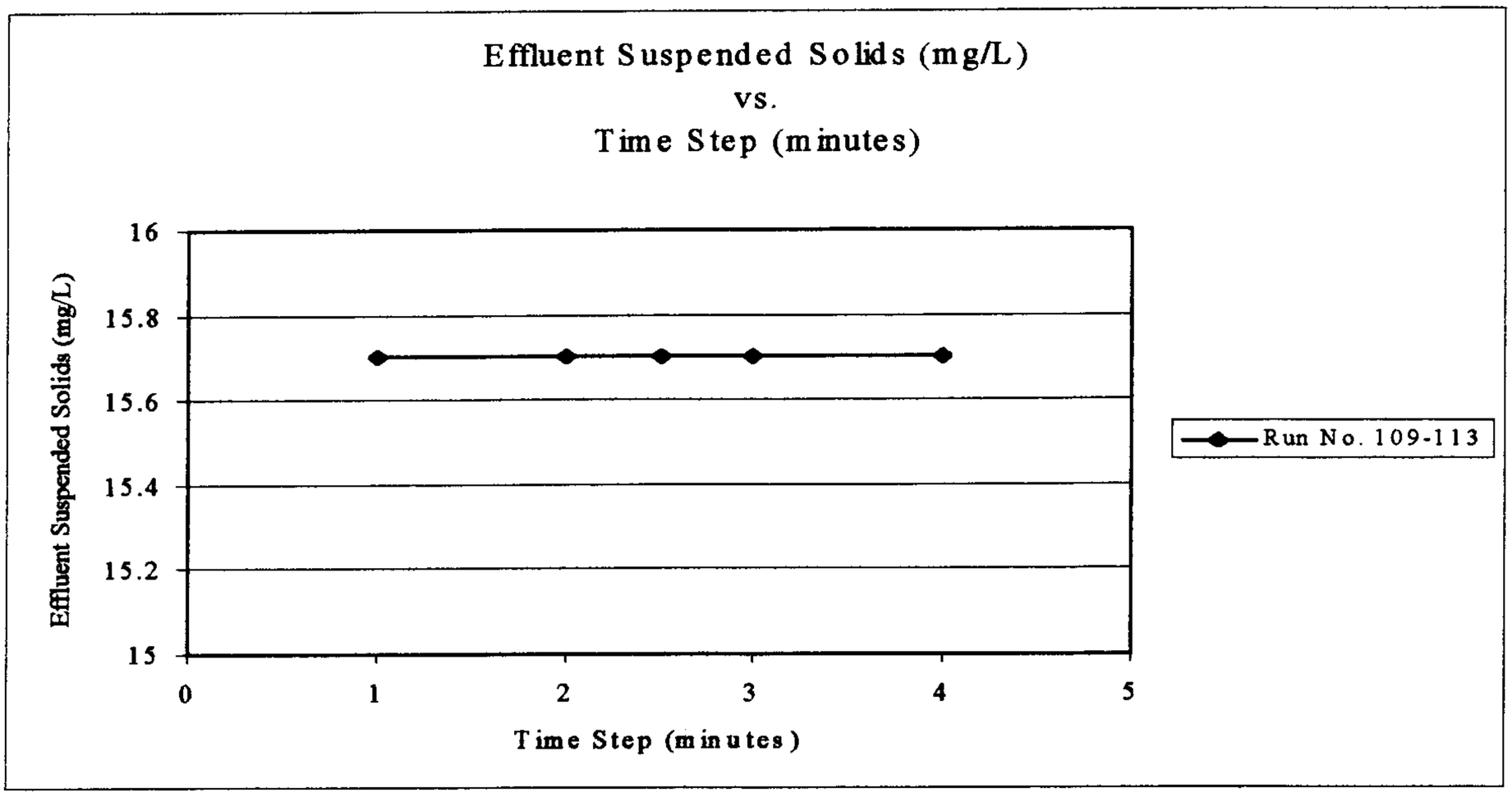

DISCUSSION

After analyzing the results, it seems that there is no clearly defined relationship between the SOR, SLR, and ESS variables for circular clarifiers. In fact, the results from this program illustrate that there are several variables that will affect a clarifier's performance, and they are all inter-related. The following discussion examines the hydraulics observed in the clarifiers and how it affected the suspended solids concentration distribution and the ESS concentration. In particular, the hydraulic issues discussed are the:

- influent hydraulics;
- recirculation zones;
- reverse sludge flow;
- sludge blanket levels; and
- effluent hydraulics.

These hydraulic flow descriptions are highly dependent on the:

- SOR;
- SLR;
- hydraulic loading (Influent + Ras);
- recirculation ratio (Ras flow / Influent flow);

- side water depth; and
- feed well skirt depth.

Influent Hydraulics

The influent hydraulics is largely governed by the hydraulic loading, which is the sum of the influent and the RAS flow per unit clarifier surface area, since this is the flow actually entering through the influent feed well. The clarifier geometry, such as the side water depth and the feed skirt depth also affect the influent hydraulics.

When the influent process flow enters a clarifier, a typical suspended solids concentration ranges from 1,000 mg/L to 4,000 mg/L, which is far denser than its surrounding fluid. Because of this density difference, the influent will plummet towards the bottom of the clarifier if unimpeded. This is known as the density waterfall. This downward flow entrains some of the surrounding fluid and creates a flow recirculation pattern in the influent zone, which is defined as the space within the influent well and the feed well skirt. The magnitude of this recirculation depends on the hydraulic load and the radial position and depth of the feed well skirt. If the feed well skirt is sufficiently deep and is not close enough to impede the influent flow, then an influent recirculation zone will develop and flow counter-clockwise. If the hydraulic load increases, or if the feed well skirt is moved closer to the influent, the skirt will impinge on the influent flow. This

forces the influent stream to flow down from the skirt, thus creating a clockwise recirculation pattern.

Both of these scenarios were observed in the simulations. Simulations with a relatively low hydraulic load (and incidentally a low solids loading), had a typical density waterfall flowing down the wall adjacent to the influent well. (Simulations 1-12, 17-19, 41-48) An example of this density waterfall is provided in figure 10.

FIGURE 10.

Simulation 1 Flow Velocity Distribution at Equilibrium

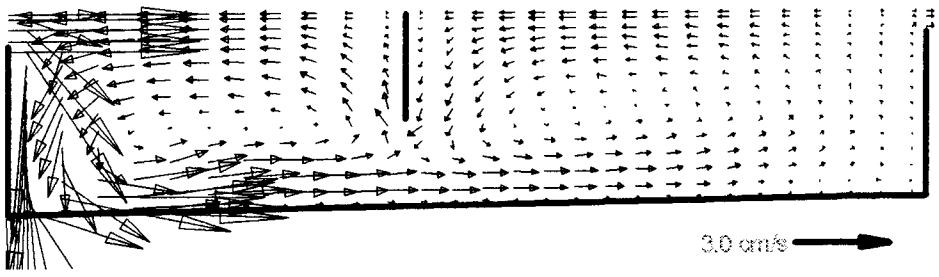

Simulations with a high hydraulic load where the influent was impinged upon by the feed well skirt were also observed. (Simulations 13-16, 22-24, 53-56, 69-72, 85-88). In the regular or shallow clarifier, this impingement resulted in a reverse recirculation. Of the deep clarifiers, a reverse recirculation in the influent zone was only observed for matrix 4, the one with the deep feed well. The other deep clarifiers had either a shallow feed well skirt or none at all. Those did not develop a reverse recirculation zone at all, and

were not sensitive in the influent zone by the high hydraulic load. An example of the reverse recirculation current is provided in figure 11.

FIGURE 11.

Simulation 13 Flow Velocity Distribution at Equilibrium

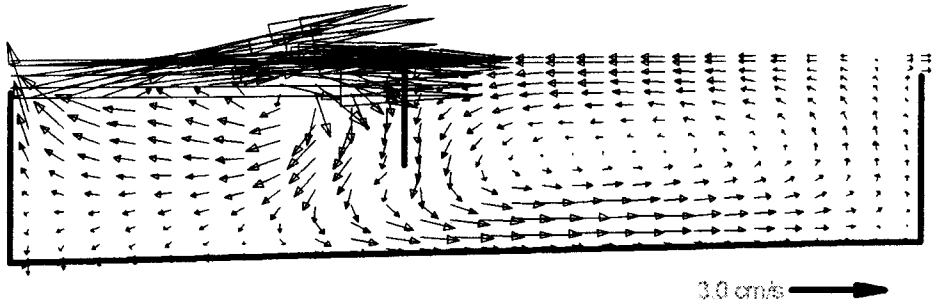

Recirculation Zones

As discussed in the previous section, the influent zone typically has either a clockwise or a counter-clockwise recirculation zone occupying most of the feedwell. In the settling zone, or effluent zone, counter-clockwise recirculation was found for most of the simulations. The only time a clockwise recirculation flow was found in the settling zone was when there were high sludge blanket levels, forcing the flow from the influent zone upwards. In the deep clarifier with the deep feed well skirt, the recirculation flow in the settling zone was very weak (Simulations 41-46), compared to the magnitude of the recirculation zone in the regular clarifiers (Simulations 1-40). For the deep clarifiers with shallow skirts, or none at all, there is only one recirculation flow pattern going around the entire tank.

It appeared that for the influent flows that did not impinge on the baffle, the influent waterfall would develop a counter-clockwise recirculation pattern and would also entrain water from the settling zone. Fluid on the settling zone side of the feed well skirt would flow down the skirt, under it, and into the recirculation eddy occupying the influent zone (Simulations 1-12, 17-19, 41-48). The entrainment of fluid from the settling zone into the influent zone can be noticed in figure 10.

Reverse Sludge Flow

The simulation results suggest that a primary reason for clarifier failure is from excessive turbulence and scour in the influent region. From viewing all of the failing simulation results, one flow pattern they all have in common is a reverse sludge flow.

In most of the simulations, the influent waterfall plummets to the clarifier bottom and flows radially outward along the clarifier bottom. In the simulations where the clarifier performed well, this solids layer flowed smoothly and slowly outward in the radial direction along the clarifier bottom, so it did not entrain very much fluid or resuspend the settled solids. In the cases where the simulations failed, there was always a layer of sludge on the clarifier bottom flowing towards the center. This reverse sludge current would not only produce turbulence along the radial length of the clarifier, it would interfere with the influent density current flowing the opposite direction. As the two

currents come together, the influent density current is redirected back upwards and toward the center of the tank as illustrated in figure 12. (Simulation 4, 8, 11, 12, 56, 16, 21, 28, 31, 32, 35, 36, 38-40, 48, 52, 56, 59, 60, 64, 76, 80, 84) This creates turbulence and hinders settling.

FIGURE 12.

Simulation 8 Flow Velocity Distribution at Equilibrium

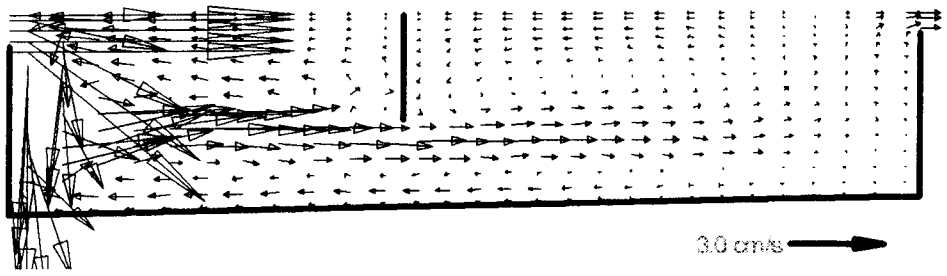

When looking at suspended solids concentration contours, the sludge blanket is clearly higher in the influent zone when this reverse sludge current exists, than when there is no reverse current. For these simulations, the sludge blanket does not reach equilibrium, continues moving upward, and eventually spills over the effluent weirs if given enough time. The simulations suggest that the presence of a steady upward flow resuspends or scours the sludge blanket. The concentration distributions and velocity profiles in appendix 2 provide a typical illustration of how this occurs.

The only explanation that the author can offer for why this reverse sludge current develops has to do with its correlation with the return activated sludge (RAS) flow. In all 16 simulations in matrix 1, the recirculation ratio (RAS flow / Influent flow) ranged from 0.31 to 3.71. Of the six simulations that did not reach equilibrium, all had a recirculation ratio of less than or equal to 0.51, with an average of 0.37. All of the simulations with a recirculation ratio greater than 0.51 were stable, regardless of the surface overflow or solids loading rate. This suggests that the RAS flow rate is a key element in keeping the sludge blanket low, and thus, preventing a clarifier from failing. If the RAS flow rate is too low, the sludge blanket is not able to achieve an adequate "compression" so that enough solids will be removed from the tank with the low RAS flow rate. When this happens, solids accumulate in the clarifier, and the sludge blanket subsequently rises and begins flowing downhill, with the aid of gravity towards the center of the clarifier. Even though increasing the RAS flow rate will increase the solids loading, the clarifier may still be able to handle a higher solids load, provided that there is not an excessively high sludge blanket. Table 9 below calculates the solids accumulation for the simulations with the shallow clarifier while figure 10 plots the results. Table 10 and figure 11 provides the same analysis for the deep clarifier

TABLE 9.

Simulation Matrices 1 and 2 Mass Balance

Run No.	Influent Flow (m^3/hr)	SOR (m/hr)	Effluent Velocity (cm/s)	MLSS (mg/L)	RAS Flow (m^3/hr)	RAS Concen-tration (mg/L)	Recirculation Ratio (RAS/INF)	Mass In (kg/hr)	RAS Mass Out (kg/hr)	Accum-ulation (kg/hr)
1	503	0.35	0.23	2363	729	3990	1.45	2911	2909	3
2	746	0.52	0.34	2363	486	5980	0.65	2911	2906	5
3	869	0.61	0.39	2363	364	7970	0.42	2911	2901	10
4	914	0.64	0.43	2363	317	7890	0.35	2911	2501	410
5	757	0.53	0.34	2363	1092	4000	1.44	4369	4368	1
6	1120	0.78	0.51	2363	729	5980	0.65	4369	4359	10
7	1303	0.91	0.59	2363	546	7670	0.42	4369	4188	181
8	1412	0.99	0.64	2363	439	7780	0.31	4369	3415	954
9	524	0.37	0.24	2363	1942	3000	3.71	5827	5826	1
10	1301	0.91	0.59	2363	1164	4990	0.89	5827	5808	19
11	1634	1.14	0.74	2363	831	7120	0.51	5827	5917	-90
12	1819	1.27	0.82	2363	647	7620	0.36	5827	4930	897
13	655	0.46	0.30	2363	2428	3000	3.71	7283	7284	-1
14	1626	1.14	0.74	2363	1456	4980	0.90	7283	7251	32
15	2043	1.43	0.93	2363	1039	6736	0.51	7283	6999	284
16	2241	1.57	1.02	2363	841	6990	0.38	7283	5879	1404
17	655	0.46		2363	158	8530	0.24	1921	1348	573
18	655	0.46		2363	584	5010	0.89	2928	2926	2
19	655	0.46		2363	1262	3580	1.93	4530	4518	12
20	655	0.46		2363	2366	3010	3.61	7139	7122	17
21	1626	1.14		2363	536	8090	0.33	5109	4336	773
22	1626	1.14		2363	631	8020	0.39	5333	5061	273
23	1626	1.14		2363	1262	5380	0.78	6824	6790	35
24	1626	1.14		2363	1940	4330	1.19	8426	8400	26

FIGURE 13.

Simulation Matrices 1 and 2 Sludge Accumulation

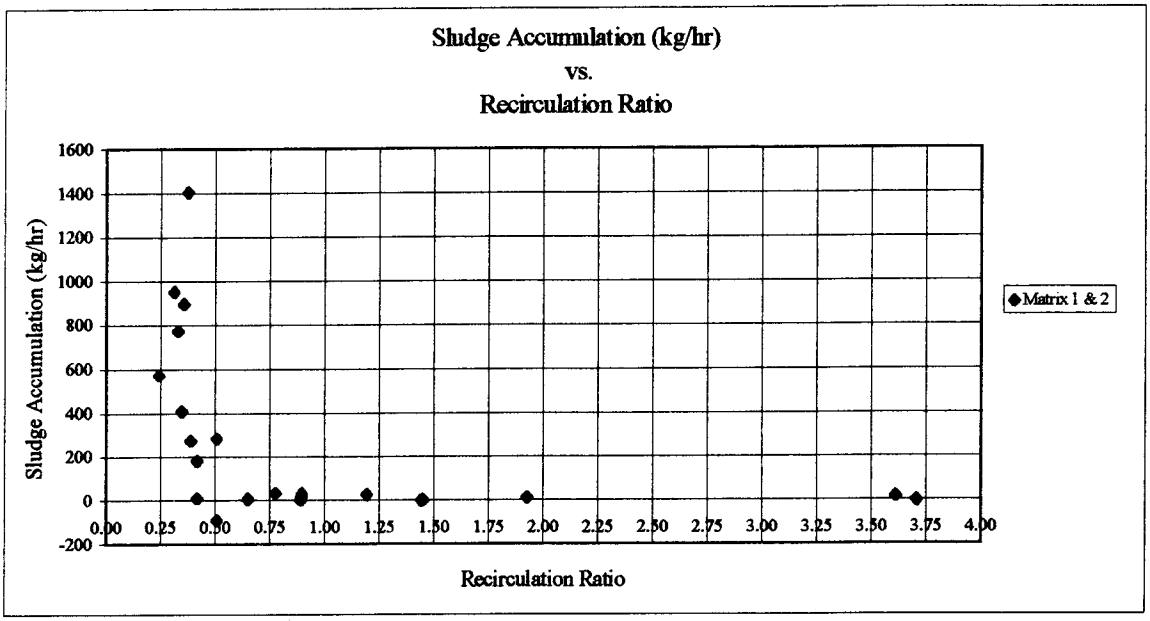

TABLE 10.

Simulation Matrices 4-6 Mass Balance

Run No.	Influent Flow (m^3/hr)	SOR (m/h)	Effluent Velocity (cm/s)	MLSS (mg/L)	RAS Flow (m^3/hr)	RAS Concen-tration (mg/L)	Recirculation Ratio (RAS/INF)	Mass In (kg/hr)	RAS Mass Out (kg/hr)	Accum-ulation (kg/hr)
41	503	0.35		2363	729	3990	1.45	2911	2909	3
42	746	0.52		2363	486	5970	0.65	2911	2901	10
43	869	0.61		2363	364	7900	0.42	2911	2876	35
44	914	0.64		2363	317	8920	0.35	2911	2828	83
45	757	0.53		2363	1092	4000	1.44	4369	4368	1
46	1120	0.78		2363	729	5980	0.65	4369	4359	10
47	1303	0.91		2363	546	7990	0.42	4369	4363	7
48	1412	0.99		2363	439	8590	0.31	4369	3771	598
49	524	0.37		2363	1942	3000	3.71	5827	5826	1
50	1301	0.91		2363	1164	4990	0.89	5827	5808	19
51	1634	1.14		2363	831	6550	0.51	5827	5443	384
52	1819	1.27		2363	647	8710	0.36	5827	5635	192
53	655	0.46		2363	2428	3000	3.71	7283	7284	-1
54	1626	1.14		2363	1456	4980	0.90	7283	7251	32
55	2043	1.43		2363	1039	6670	0.51	7283	6930	353
56	2241	1.57		2363	841	7260	0.38	7283	6106	1177
57	503	0.35		2363	729	3990	1.45	2911	2909	3
58	746	0.52		2363	486	5930	0.65	2911	2882	29
59	869	0.61		2363	364	7690	0.42	2911	2799	112
60	914	0.64		2363	317	8530	0.35	2911	2704	207
61	757	0.53		2363	1092	4000	1.44	4369	4368	1
62	1120	0.78		2363	729	6010	0.65	4369	4381	-12
63	1303	0.91		2363	546	8040	0.42	4369	4390	-21
64	1412	0.99		2363	439	9740	0.31	4369	4276	93
65	524	0.37		2363	1942	3000	3.71	5827	5826	1
66	1301	0.91		2363	1164	5000	0.89	5827	5820	7
67	1634	1.14		2363	831	6920	0.51	5827	5751	76
68	1819	1.27		2363	647	8810	0.36	5827	5700	127
69	655	0.46		2363	2428	3000	3.71	7283	7284	-1
70	1626	1.14		2363	1456	4990	0.90	7283	7265	17
71	2043	1.43		2363	1039	6970	0.51	7283	7242	41
72	2241	1.57		2363	841	8630	0.38	7283	7258	25
73	503	0.35		2363	729	3990	1.45	2911	2909	3
74	746	0.52		2363	486	5960	0.65	2911	2897	15
75	869	0.61		2363	364	7770	0.42	2914	2828	85
76	914	0.64		2363	317	8950	0.35	2909	2837	72
77	757	0.53		2363	1092	4000	1.44	4369	4368	1
78	1120	0.78		2363	729	6010	0.65	4369	4381	-12
79	1303	0.91		2363	546	8180	0.42	4369	4466	-97
80	1412	0.99		2363	439	9060	0.31	4374	3977	397
81	524	0.37		2363	1942	3000	3.71	5827	5826	1
83	1634	1.14		2363	831	6940	0.51	5825	5767	58
84	1819	1.27		2363	647	8430	0.36	5827	5454	373
85	655	0.46		2363	2428	3000	3.71	7285	7284	1
86	1626	1.14		2363	1456	4990	0.90	7283	7265	17
87	2043	1.43		2363	1039	7000	0.51	7283	7273	10
88	2241	1.57		2363	841	8750	0.38	7283	7359	-76

FIGURE 14.

Simulation Matrices 4-6 Sludge Accumulation

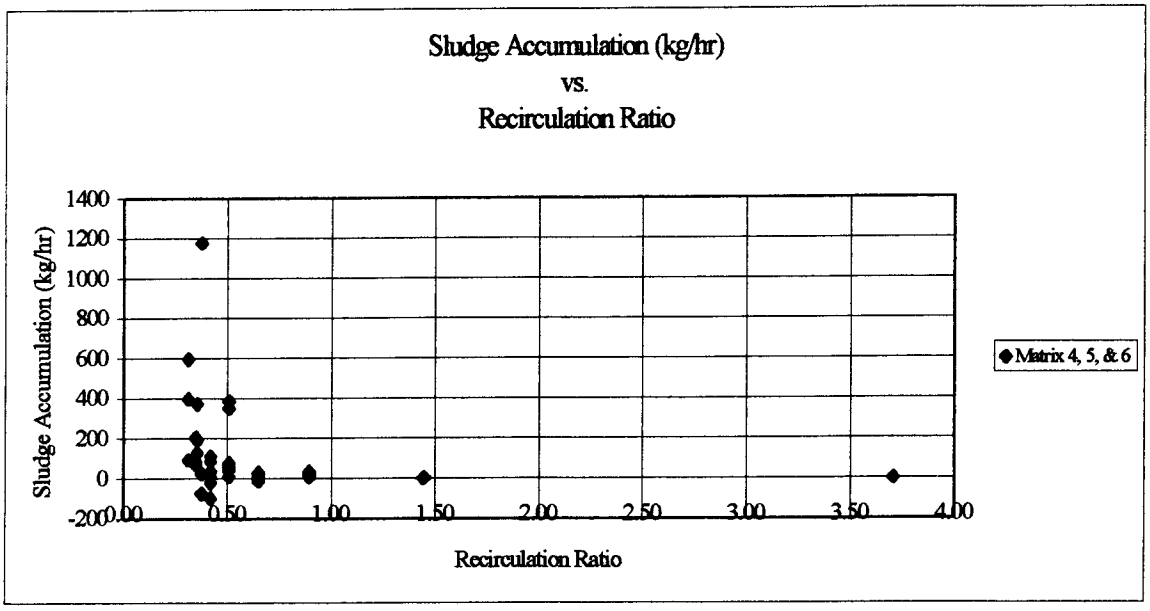

In matrices 4-6, the deeper tanks can operate without sludge accumulation at a lower recirculation ratio than the shallower tanks of matrix 1 and 2. Of the nine simulations in matrices 4-6 that did not reach equilibrium, all had a recirculation ratio of 0.42 or less, with an average of 0.35. Though not a large difference, these findings suggest that deeper tanks have more room to store accumulated sludge, and can operate adequately with a lower recirculation ratio (or lower sludge withdrawal rate).

Sludge Blanket Levels

The presence of a high sludge blanket will inevitably mean failure for the clarifiers simulated. As the sludge blanket moves higher, there is less of a scouring effect from the influent density waterfall since it has less energy (the greater the fall distance, the higher the influent waterfall potential energy). However, if a feed well baffle is present and the sludge blanket levels are high, the flow is "pinched," or forced under the baffle at a higher velocity, which then further scours the sludge blanket and resuspends the solids. Also, even though the magnitude of the scouring is not as great when the influent waterfall has less distance to travel before encountering the sludge blanket, the scouring occurs at a higher elevation, and consequently closer to the effluent weir. When this happens, the resuspended solids have less of a travel distance to the effluent weirs, which sometimes translates to higher ESS concentrations.

Simulations 16, 32, 36, 39, and 40 all have high sludge blanket levels, which cause the influent flow to become pinched upward, as is shown in the corresponding figures in the appendix and in figure 12 below. When the flow is pinched upward, in some cases it creates a short-circuiting flow-path to the effluent weirs. In others, it creates additional recirculation zones that are highly unstable to develop in the settling zone. In simulations 32 and 39, three recirculation zones were created in the settling zone, which increases the amount of scour.

FIGURE 15.

Simulation 39 Flow Velocity Distribution at Equilibrium

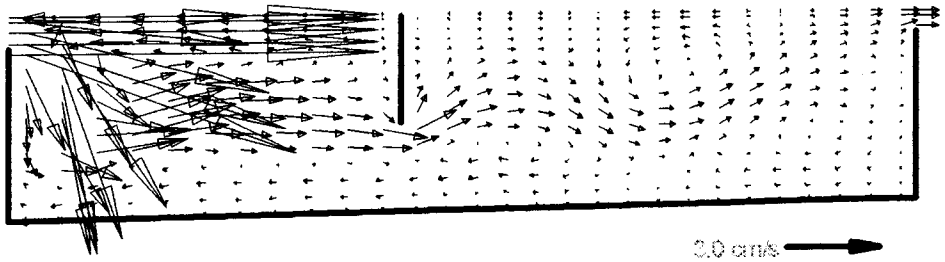

Effluent Hydraulics

Researchers and engineers studying clarifiers have long proposed that the effluent suspended solids concentration is highly sensitive to the effluent hydraulics. Upon viewing the velocity profiles in the simulations, it is clear that the model predicts a greater fluid velocity in the effluent zone as the SOR increases. There is a very strong correlation between the effluent fluid velocity and the SOR. Figure 13 plots the fluid velocity over the effluent weirs versus the SOR. The results are a strongly linear correlation, which has a statistical R squared value of 0.9998. This is expected because of the continuity condition imposed in the solution. The volume of fluid (minus the RAS flow) must equal the volume flowing over the effluent weirs.

FIGURE 16.

Simulation Matrix 1

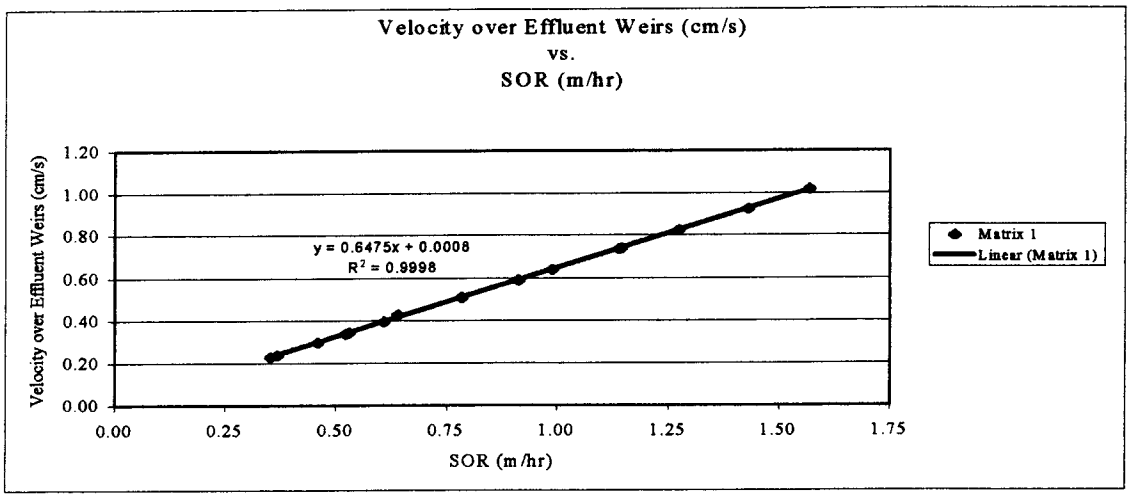

However, like the SOR, the results do not suggest a strong correlation between the effluent fluid velocity and the ESS concentration for all the simulations. Simulations in matrix 1 and 4 certainly do not suggest a correlation. Some field tests in the past have suggested the ESS concentration is dependent on the effluent zone hydraulics, yet the simulation results do not provide support or disagreement with this correlation. It appears that the ESS concentration is more sensitive to other parameters such as the solids loading, RAS flow rate, and the location and magnitude of recirculation zones that induce sludge blanket scouring.

Effect of Clarifier Geometry on ESS

Figures 13-16, which graph the ESS vs. SOR for the four different clarifier geometries show the ESS concentration to be sensitive to the geometries at the low solids loading rate of 2.04 kg/m^2/hr and at the higher solids loading rates of 4.08 and 5.10 kg/m^2/hr. Interestingly, for the lowest solids loading rate of 2.04 kg/m^2/hr, the shallow clarifier performed better than the deep clarifiers by about 2-6 mg/L.

FIGURE 17.

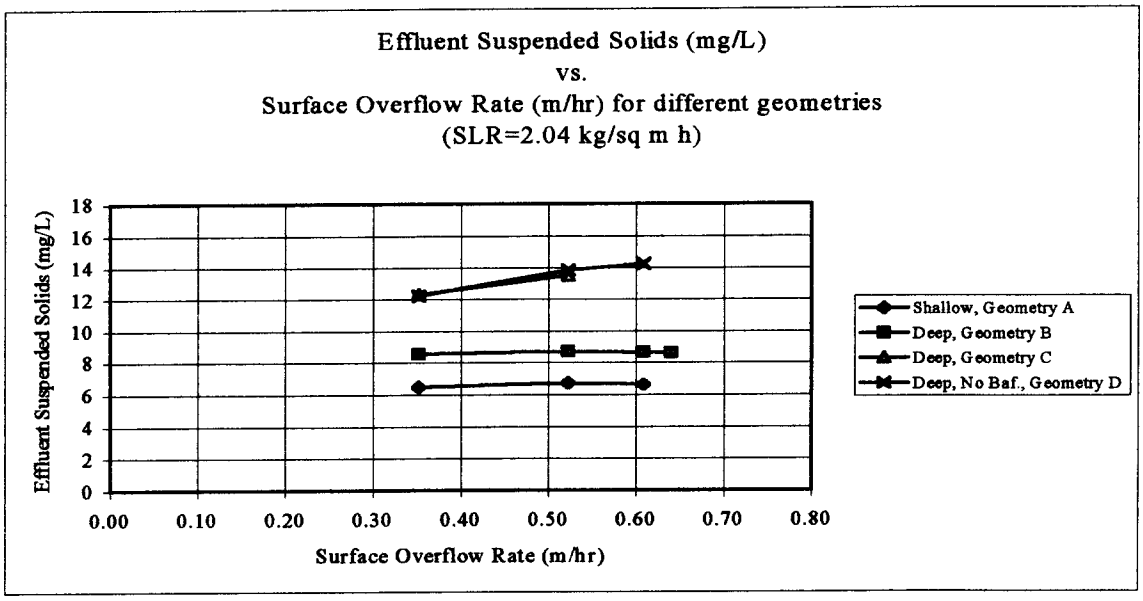

For the solids loading rate of 3.06 kg/m^2/hr, there is very little dependence on the geometry since all of the results are within 1 mg/L of 8 mg/L.

FIGURE 18.

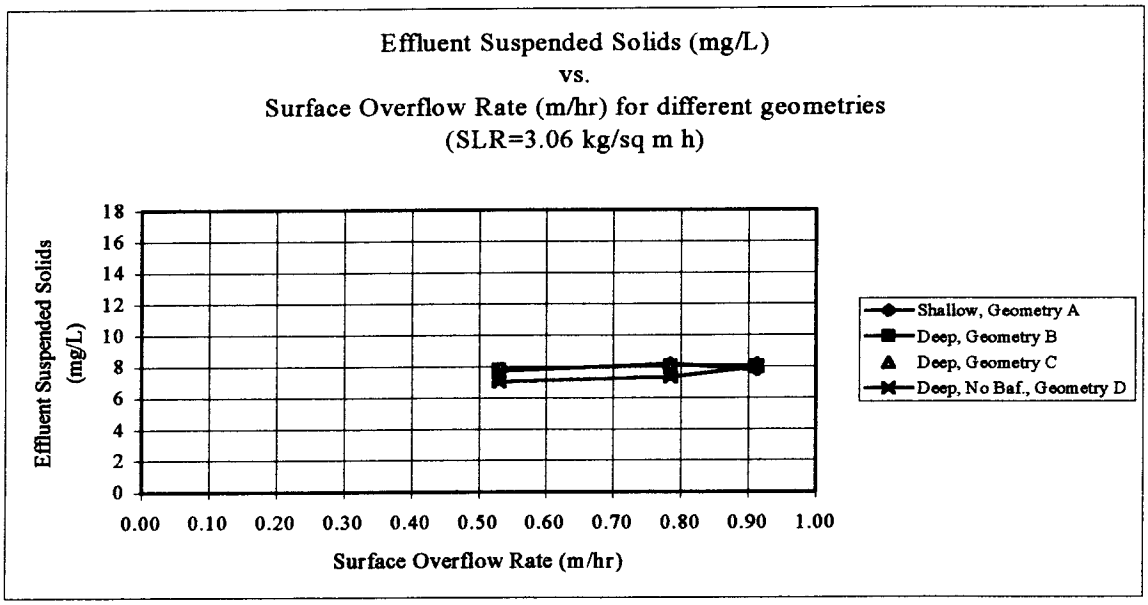

For the solids loading rate of 4.08 kg/m^2/hr, a small separation develops in the ESS concentration for the different geometries. The shallow clarifier has the highest ESS concentration for this solids loading rate. Then, geometry B, C, and D follow closely, mostly in that order. As the SOR nears 1.5 m/hr, the ESS concentration for the different geometries converges to about 12 mg/L.

FIGURE 19.

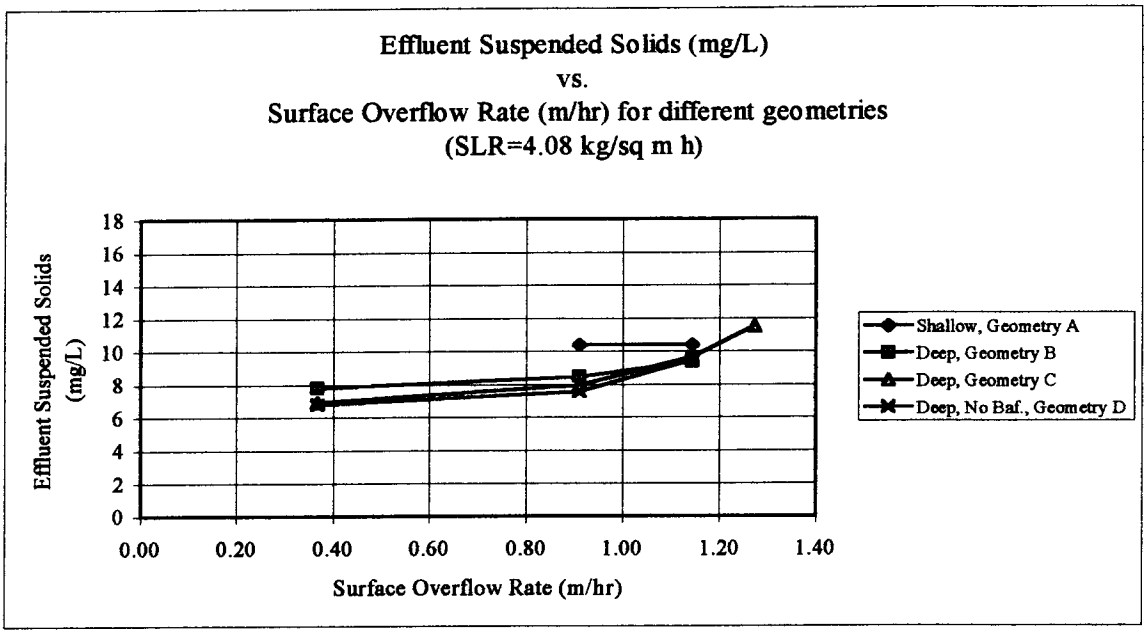

For the solids loading rate of 5.10 kg/m^2/hr, the separation in the ESS concentration is larger than the separation for the simulations at a lower SLR. The concentration converges to 16 mg/L as the SOR increases to near 1.5 m/hr. The deep clarifier with the deepest baffle has the worst efficiency throughout the range of SOR simulated, and is closely followed by the shallow clarifier with an ESS concentration ranging from 12-16 mg/L for those simulations that did not fail. The deep clarifier with the shallow skirt and the deep clarifier with no baffles provide follows with an ESS concentration ranging from 8-16 mg/L.

FIGURE 20.

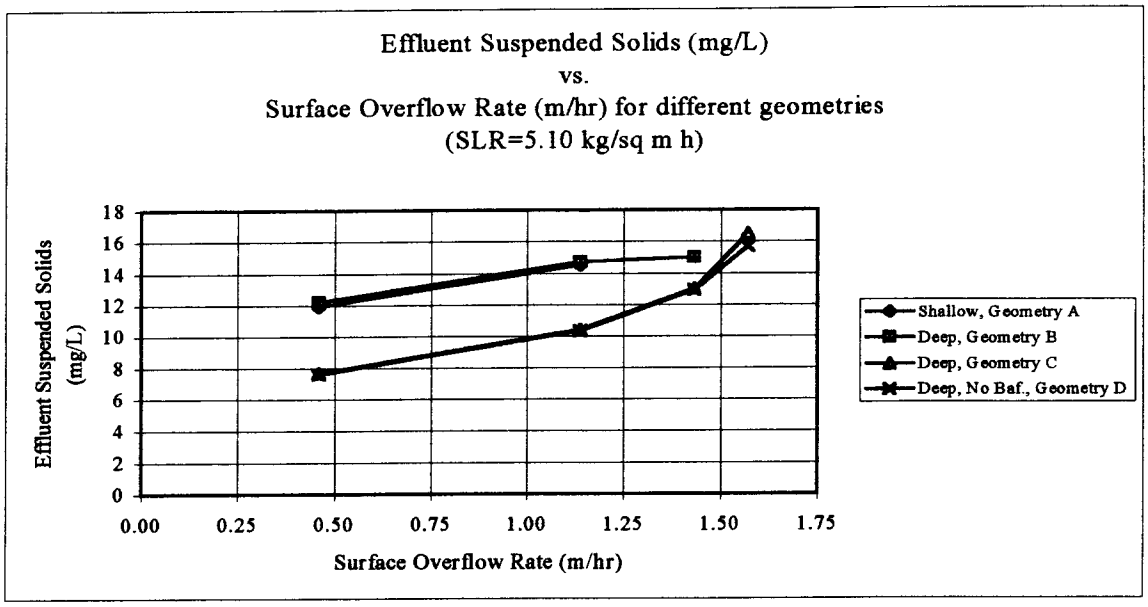

A few geometry-related trends that the simulations suggest are:

- At low to medium solids loading rates, the shallow clarifier performs as well or better than the deep clarifiers in terms of ESS concentration.
- At low to medium solids loading rates applied to the deep clarifiers, the clarifier with the deepest feed skirt has the best performance within the tested range.
- At higher solids loading rates, the deep clarifier with no baffles has the best performance. Also, the deep clarifier with no baffles seems to be more stable in terms of reaching equilibrium.

OTHER CONSIDERATIONS

Failure

All of the clarifiers, except for those in matrix 3 were not overloaded based on a state-point analysis. This type of analysis predicted that none of the simulations should have failed; yet many did. The inability of state-point analysis to predict failure has also been noted by others in clarifier investigations. Ekama and Morris (1986) showed that failure occurred at 80% of the limiting solids flux predicted by a state-point analysis for 45 stress tests on 22 different clarifiers. Also, in a study by Watts *et al.* (1996), overloaded conditions were found at 73% to 91% of the limiting solids flux predicted by a state point analysis.

Perhaps the main reason why a state-point analysis did not predict the failures that occurred in the simulations can be explained by the lack of any hydrodynamic consideration in a state-point analysis. When performing a state-point analysis, a settling flux curve is generated from the known solid's settling properties. On this flux curve, a geometrical analysis is performed with two lines. One has positive slope equal to the SOR, and the other has a negative slope equal to the RAS flow rate divided by the clarifier surface area. The line corresponding to the RAS flow rate is positioned to intersect with the other line at the vertical co-ordinate equal to the solids flux into the clarifier. Where this intersection of the two lines falls and the position of the two lines in

relation to the settling flux curve determines if a clarifier is overloaded or not. Other than these three parameters, there is no consideration for any hydrodynamic effects that may improve or hinder the settling process. The results from these simulations clearly demonstrate that hydrodynamic effects such as flow recirculation, short-circuiting, baffle impingement, or a reverse sludge flow along the clarifier bottom significantly impact a clarifier's performance. This type of observation can be made with extensive amounts of field data, or with the aid of computer modeling.

Another reason why some of these simulations failed may be explained by how a clarifier behaves in real life. In real clarifiers, there is a dynamic coupling between the activated sludge aeration basin and the clarifier. When they are in equilibrium with each other, a uniform amount of solids flow into the clarifier and a uniform amount of solids are withdrawn from the clarifier. When a clarifier is overloaded, the solids concentration in the aeration tank will decrease. An overloaded clarifier cannot settle and thicken the influent solids quickly enough, and will accumulate solids throughout the tank in the form of a rising sludge blanket. When this happens, the solids are not being thickened adequately in the clarifier, therefore, the RAS flow going back into the aeration basin will have a lowered solids concentration. This will inevitably lower the mixed-liquor solids concentration, which will in turn, lower the solids loading into the clarifier. If the clarifier is deep enough, it will have enough sludge storage volume available to accommodate the rising sludge blanket without having too adverse an impact on the ESS concentration. If the tank is shallow and does not have adequate storage volume, a

significant quantity of solids will flow over the effluent weirs until the system reaches equilibrium again.

The clarifier model used here did not take into account this coupling with the aeration basin. Most of the simulations that failed did so because of a rising sludge blanket. After 600 minutes, the ESS concentration was usually acceptable, but it was clear that if given enough time, the sludge blanket would rise up and over the effluent weirs. A few simulations were allowed to run until this occurred. The ESS concentration would reach equilibrium after 2,000 minutes of simulation time at a concentration of 200-600 mg/L. Clearly, in a real life situation, this gross discharge of solids in the effluent would not continue as is suggested by the model. More recent work by the creators of the program (Zhong *et al.* 1996) has begun incorporating this coupling effect into their programs.

Suggestions for Upgrading Model

The version used here was the first of a series of versions put forth by the program's creators. It has shown to be very easy to use due to the user-friendly windows-type interface. The program allows the user to investigate the effects changing one parameter will have while keeping all other constant. Here lies a significant difference between computer modeling and field-testing. In field testing, it is very difficult to isolate a parameter, as can be done with computer models. Field-testing has made significant advances in understanding clarifier behavior and will continue to do so. Also, field-

testing is crucial for evaluating a model's predictive powers since data obtained from properly performed field tests is "real." However, with recent clarifier models that can accurately model "real" clarifiers, computer modeling is becoming a very powerful tool for clarifier analysis. As the processing speed of new computers increases, three-dimensional modeling will become more feasible, and such modeling programs will become even more realistic.

Following are some suggestions that the author feels would greatly enhance this program:

- Clarifier dye testing is a relatively easy test to perform and is a very popular method in examining a clarifier's hydraulic efficiency. Even though there are shortcomings in this method, it remains the most common experiment for evaluating a clarifier's hydrodynamics. The addition of a dye tracer simulation could be very helpful for evaluating a real-life tracer study. If the model's tracer results correspond closely with the actual results, the user could look at the velocity and solids distribution to identify where the possible problem areas are. With the program's current configuration, a tracer simulation could be conducted for a neutral-density situation by setting the settling velocity very near zero and varying the influent concentration to simulate that of a slug or a step. Unfortunately, secondary clarifiers have stratified flow, so a tracer simulation performed this way is not realistic.

- The program uses the settling equation of Takacs *et al.* (1991). One of the variables in this equation is C_{min}, which is defined as the concentration of non-settleable particles. The program uses a C_{min} as 0.2% of the influent concentration for all simulations. The user can not readily adjust this parameter. If the program creators continue to use this equation for a settling model, the program user should be able to change this parameter as a calibration tool.

- An even better improvement to the program would be to eliminate the need to calibrate the solids settling properties. A problem associated by calibrating the C_{min} parameter to the physically measured minimum suspended solids concentration is the user may inadvertently be including the effects of imperfect clarifier design and operation.

- As mentioned earlier, coupling the clarifier model with an activated sludge aeration basin would greatly increase the utility of the model. There were several simulations which failed in this investigation, yet likely, would not have in "real life." Coupling the clarifier

with an aeration basin would simulate the dynamic interplay that occurs between a clarifier and aeration basin to bring an overloaded clarifier back into equilibrium.

Future Work

Computer models that can accurately model a clarifier provide an excellent opportunity for exploring how specific variables affect a clarifier's efficiency. A good problem, which still has engineers and researchers at odds, is how deep a clarifier needs to be. There are certainly advantages to having a deep clarifier; the most important being that there is added volume for sludge storage. However, building a deep clarifier is more expensive than a shallower one, and the results here suggest that at lower solids and hydraulic loading rates, a shallower clarifier actually provides better suspended solids removal efficiency. It is unclear from these simulations if this is a result of the hydraulic or solids loading, since they are closely coupled. More than likely, it is a result of a hydraulic mechanism.

Another issue which deserves more exploration is the sludge thickening. This has been studied before, but only recently with a coupled model with a clarifier submodel as sophisticated as the one used here (Zhong *et al.* 1996). Zhong *et al.* examined the affect of varying the RAS flow rate had on other process variables. The next step may be repeating the same exercise with different clarifier geometries. This may help quantify the degree to which the clarifier hydraulics improve or degrade the thickening process.

CONCLUSIONS

For circular clarifiers, these simulations suggest that for certain loading and geometrical conditions, the ESS concentration is virtually independent of the SOR loading and is far more sensitive to the solids loading rate.

- In particular, the shallow clarifier was most sensitive to the solids loading rate at SOR loadings at or below 1 m/hr (600 gal/ft^2/d). As the SOR increases past 1 m/hr, the ESS concentration would then increase as well.
- The deep clarifier with the deepest baffle provided similar results. For this configuration, the ESS was not sensitive to the SOR loading throughout the entire range tested of 0.35 m/hr (215 gal/ft^2/d) to 1.5 m/hr (925 gal/ft^2/d).

It appears that the common condition between these two simulation sets is that the feed well skirt extended a little more than half way through the depth of the clarifier. In the simulations of the deep clarifier with none or a short feed well skirt, the results were quite different.

- For the deep clarifiers with a short or non-existent feed well skirt, the ESS concentration was quite sensitive to the SOR, and weakly sensitive to the solids loading rate.

A comparison between the shallow and deep clarifier simulations gives an interesting result. For low hydraulic and solids loading rates of 2.04 kg/m^2/hr and 3.06 kg/m^2/hr (10.5 lb/ft^2/d and 15.7 lb/ft^2/d), the shallow clarifier produces a higher quality effluent; 0-6 mg/L better than the deep clarifier. However, under the higher solids loads of 4.08

kg/m^2/hr and 5.10 kg/m^2/hr (20.9 lb/ft^2/d and 26.2 lb/ft^2/d), the deep clarifier performs significantly better than the shallow clarifier by about 0-5 mg/L. Perhaps this can be explained by the greater potential energy the influent waterfall has in a deep clarifier. This energy translates to more scouring of the sludge blanket.

Many of the simulations performed did not reach equilibrium and had a rising sludge blanket. The primary reason for this failure seemed to be a low RAS recirculation ratio. Most of the simulations with a recirculation ratio less than about 0.4 failed due to a rising sludge blanket. The solids did not settle and thicken quickly enough to be withdrawn from the clarifier and returned to the aeration basin. The simulations with a recirculation ratio above 0.5 were very stable, even with a high surface overflow or solids loading rate. A result of the increasing sludge blanket was a reverse sludge flow, which caused more turbulence in the influent zone as it met the influent waterfall. This increased the scouring, and raised the sludge blanket even higher.

Another possible reason why some of the simulations failed at what seemed like low loading rates is that this model is un-coupled with the preceding aeration basin. In a real clarifier, solids accumulate in an overloaded clarifier, which reduces the solids mass returning to the aeration basin, which in turn lowers the solids loading on the clarifier. This dynamic relationship can prevent a clarifier from developing a rapidly rising sludge blanket. While the ESS concentration may contain an elevated solids concentration in this scenario, it does not necessarily mean that the sludge blanket will rise to the top and

stay there. To predict the ESS concentration of a clarifier that is operating near its limit, a coupled model will perform better than an un-coupled one.

REFERENCES

Adams, E.W., and W. Rodi. 1990. Modeling Flow and Mixing in Sedimentation Tanks. Journal of Hydraulic Engineering, Vol. 116, No. 7, pp. 895-913.

Albertson, O.E., and J.P. Wilson. 1997. Clarifier Design Concept – Larger is Better. Journal of Environmental Engineering, Vol. 123, No. 11, pp. 1159-1161.

Camp, T.R. 1945. Sedimentation and the Design of Settling Tanks. Proceedings of the American Society of Civil Engineers, April 1945, pp. 895-958.

Celik, I. And W. Rodi. 1985. Prediction of Hydrodynamic Characteristics of Rectangular Settling Tanks. International Symposium on Refined Flow Modeling and Turbulence Measurements. Iowa City, Iowa, U.S.A., pp. 641-651.

Clifft, R.C. 1980. A Dynamic Model for Predicting Oxygen Utilization in Activated Sludge Processes. Ph.D. dissertation, Department of Civil Engineering, University of Houston, Texas, U.S.A.

Clifft, R.C. and J.F. Andrews. 1981. Predicting the Dynamics of Oxygen Utilization in the Activated Sludge Process. Journal. Water Pollution Control Federation, Vol 53, pp. 1219-1232.

Dobbins, W.E. 1943. Effect of Turbulence on Sedimentation. Proceedings of the American Society of Civil Engineers, February 1943, pp. 629-678.

Dupont, R. and M. Henze. 1992. Modeling of the Secondary Clarifier Combined with the Activated Sludge Model No. 1. Water Science Technology, Vol. 25, pp. 285-300.

Gosman, A.D. and W.M. Pun. (1974). Lecture Notes for Calculating Recirculating Flows. HTS/74/2, Imperial College, London, England

Imam, E., and J.A. McCorquodale. 1983. Simulation of Flow in Rectangular Clarifiers. Journal of Environmental Engineering, Vol. 109, No. 3, pp. 713-730.

Keinath, T.M. 1985. Operational Dynamics and Control of Secondary Clarifiers. Journal Water Pollution Control Federation, Vol. 57, No. 7, pp. 770-776.

Larsen, P. 1977. On the Hydraulics of rectangular Settling Basins, Experimental and Theoretical Studies. Report No. 1001, Department of Water Resources Engineering, Lund Institute of Technology, Lund, Sweden.

Launder, B.E., and D.B. Spalding. 1974. The Numerical Computation of Turbulent Flows. Computer Methods in Applied Mechanics and Engineering, Vol. 3, pp. 269-289.

Lyn, D.A., and W. Rodi. 1990. Turbulence Measurements in Model Settling Tank. Journal of Hydraulic Engineering, Vol. 116, No. 1, pp. 3-21.

McCorquodale, J.A., and S. Zhou. 1993. Effects of Hydraulic and Solids Loading on Clarifier Performance. Journal of Hydraulic Research, Vol. 31, No. 4, pp. 461-477.

Ostendorf, D.W. 1986. Hydraulics of Rectangular Clarifiers. Journal of Environmental Engineering. Vol. 112, No. 5, pp. 939-952.

Patankar, S.V. and D.B. Spalding. 1972. A Calculation Procedure for Heat, Mass, and Momentum Transfer in Three-Dimensional Parabolic Flow. International Journal of Heat and Mass Transfer, Vol. 15, pp. 1787.

Patankar, S.V. 1980. Numerical Heat Transfer and Fluid Flow. McGraw-Hill Inc., New York, N.Y., U.S.A.

Patry, G. and I. Takacs. 1992. Settling of Flocculent Suspensions in Secondary Clarifiers. Journal of Water Research, Vol. 26, No. 4, pp. 473-479.

Samstag, R.W., D.F. Dittmar, Z. Vitasovic, and J.A. McCorquodale. 1992. Underflow Geometry in Secondary Sedimentation. Water Environment Research, Vol. 64, No. 3, pp. 204-212.

Schamber, D.R., and B.E. Larock. 1981. Numerical Analysis of Flow in Sedimentation Basins. Proceedings of the American Society of Civil Engineers, Hydraulics Division, Vol. 107, No. HY5, pp. 575-591.

Stamou, A.I., E.W. Adams, and W. Rodi. 1989. Numerical Modeling of Flow and Settling in Primary Rectangular Clarifiers. Journal of Hydraulic Research, Vol. 27, No. 5, pp. 665-682.

Stenstrom, M.K. 1976. A Dynamic Model and Computer Compatible Control Strategies for Wastewater Treatment Plants. Ph.D. thesis, Clemson University, Clemson, South Carolina, U.S.A.

TeKippe, R.J., and J.L. Cleasby. 1968. Model Studies of a Peripheral Feed Settling Tank. Proceedings of the American Society of Civil Engineers, Vol. 94, No. SA1, pp. 85-102.

Vitasovic, Z.C. 1989. Continuous Settler Operation: A Dynamic Model. In Dynamic Modeling and Expert System in Wastewater Engineering. G.G. Patry, and D. Chapman (Eds.), Lewis Publishers, Chelsea, Michigan, U.S.A.

Vitasovic, Z.C., S. Zhou, J.A. McCorquodale, and K. Lingren. 1997. Secondary Clarifier Analysis Using Data from the Clarifier Research Technical Committee Protocol. Water Environment Research, Vol. 69, No. 5, pp. 999-1007.

Wahlberg, E.J., H.Z. Gerges, A. Gharagozian, and M.K. Stenstrom. 1997. Discussion of: Secondary Clarifier Analysis Using Data from the Clarifier Research Technical Committee Protocol (Vitasovic *et al.* 1997).

Wahlberg, E.J., T.M. Keinath, and D. Parker. 1994. Influence of Activated Sludge Flocculation Time on Secondary Clarification. Water Environment Research, Vol. 66, No. 6, pp. 779-786.

Zhong, J., J.A. McCorquodale, S. Zhou, and Z. Vitasovic. 1996. A Dynamic Solids Inventory Model for Activated Sludge Systems. Water Environment Research, Vol. 68, No. 3, pp. 329-337.

Zhou, S., and J.A. McCorquodale. 1992a. Modeling of Rectangular Settling Tanks. Journal of Hydraulic Engineering, Vol. 118, No. 10, pp. 1391-1405.